

Manuscript Number: LITHOS6284R2

Title: Tracing subduction zone fluid-rock interactions using trace element and Mg-Sr-Nd isotopes

Article Type: Regular Article

Keywords: Mg isotopes; subduction channel; fluid-rock interaction; eclogite; Tianshan

Corresponding Author: Dr. Shuijiong Wang, Ph.D

Corresponding Author's Institution: China University of Geosciences

First Author: Shuijiong Wang, Ph.D

Order of Authors: Shuijiong Wang, Ph.D; Fang-Zhen Teng; Shu-Guang Li; Li-Fei Zhang; Jin-Xue Du; Yong-Sheng He; Yaoling Niu

Abstract: Slab-derived fluids play a key role in mass transfer and elemental/isotopic exchanges in subduction zones. The exhumation of deeply subducted crust is achieved via a subduction channel where fluids from various sources are abundant, and thus the chemical/isotopic compositions of these rocks could have been modified by subduction-zone fluid-rock interactions. Here, we investigate the Mg isotopic systematics of eclogites from southwestern Tianshan, in conjunction with major/trace element and Sr-Nd isotopes, to characterize the source and nature of fluids and to decipher how fluid-rock interactions in subduction channel might influence the Mg isotopic systematics of exhumed eclogites. The eclogites have high LILEs (especially Ba) and Pb, high initial $^{87}\text{Sr}/^{86}\text{Sr}$ (up to 0.7117; higher than that of coeval seawater), and varying Ni and Co (mostly lower than those of oceanic basalts), suggesting that these eclogites have interacted with metamorphic fluids mainly released from subducted sediments, with minor contributions from altered oceanic crust or altered abyssal peridotites. The positive correlation between $^{87}\text{Sr}/^{86}\text{Sr}$ and Pb^* (an index of Pb enrichment; $\text{Pb}^* = 2 \cdot \text{PbN}/[\text{CeN} + \text{PrN}]$), and the decoupling relationships and bidirectional patterns in $^{87}\text{Sr}/^{86}\text{Sr}$ -Rb/Sr, Pb^* -Rb/Sr and Pb^* -Ba/Pb spaces imply the presence of two compositionally different components for the fluids: one enriched in LILEs, and the other enriched in Pb and $^{87}\text{Sr}/^{86}\text{Sr}$. The systematically heavier Mg isotopic compositions ($\delta^{26}\text{Mg} = -0.37$ to $+0.26$) relative to oceanic basalts ($-0.25 \leq 0.07$) and the roughly negative correlation of $\delta^{26}\text{Mg}$ with MgO for the southwestern Tianshan eclogites, cannot be explained by inheritance of Mg isotopic signatures from ancient seafloor alteration or prograde metamorphism. Instead, the signatures are most likely produced by fluid-rock interactions during the exhumation of eclogites. The high Rb/Sr and Ba/Pb but low Pb^* eclogites generally have high bulk-rock $\delta^{26}\text{Mg}$ values, whereas high Pb^* and $^{87}\text{Sr}/^{86}\text{Sr}$ eclogites have mantle-like $\delta^{26}\text{Mg}$ values, suggesting diverse influences of the two fluid components on the Mg isotopic systematics of these eclogites. The LILE-rich fluid component, possibly derived from mica-group minerals, contains a considerable amount of heavy Mg that has shifted $\delta^{26}\text{Mg}$ of the eclogites towards higher values. By contrast, the $^{87}\text{Sr}/^{86}\text{Sr}$ - and Pb-rich fluid component, most likely released from epidote-group minerals in

metasediments, has little Mg so as not to modify the Mg isotopic composition of the eclogites. In addition, the influence of talc-derived fluid might be evident in a very few eclogites that have low Rb/Sr and Ba/Pb but slightly heavier Mg isotopic compositions. These findings represent an important step toward a broad understanding of the Mg isotope geochemistry in subduction zones, and contributing to understanding why island arc basalts have averagely heavier Mg isotopic compositions than the normal mantle.

Abstract

Slab-derived fluids play a key role in mass transfer and elemental/isotopic exchanges in subduction zones. The exhumation of deeply subducted crust is achieved via a subduction channel where fluids from various sources are abundant, and thus the chemical/isotopic compositions of these rocks could have been modified by subduction-zone fluid-rock interactions. Here, we investigate the Mg isotopic systematics of eclogites from southwestern Tianshan, in conjunction with major/trace element and Sr-Nd isotopes, to characterize the source and nature of fluids and to decipher how fluid-rock interactions in subduction channel might influence the Mg isotopic systematics of exhumed eclogites. The eclogites have high LILEs (especially Ba) and Pb, high initial $^{87}\text{Sr}/^{86}\text{Sr}$ (up to 0.7117; higher than that of coeval seawater), and varying Ni and Co (mostly lower than those of oceanic basalts), suggesting that these eclogites have interacted with metamorphic fluids mainly released from subducted sediments, with minor contributions from altered oceanic crust or altered abyssal peridotites. The positive correlation between $^{87}\text{Sr}/^{86}\text{Sr}$ and Pb^* (an index of Pb enrichment; $\text{Pb}^* = 2 \cdot \text{Pb}_N / [\text{Ce}_N + \text{Pr}_N]$), and the decoupling relationships and bidirectional patterns in $^{87}\text{Sr}/^{86}\text{Sr}$ -Rb/Sr, Pb^* -Rb/Sr and Pb^* -Ba/Pb spaces imply the presence of two compositionally different components for the fluids: one enriched in LILEs, and the other enriched in Pb and $^{87}\text{Sr}/^{86}\text{Sr}$. The systematically heavier Mg isotopic compositions ($\delta^{26}\text{Mg} = -0.37$ to $+0.26$) relative to oceanic basalts (-0.25 ± 0.07) and the roughly negative correlation of $\delta^{26}\text{Mg}$ with MgO for the southwestern Tianshan eclogites, cannot be explained by inheritance of Mg isotopic signatures from

ancient seafloor alteration or prograde metamorphism. Instead, the signatures are most likely produced by fluid-rock interactions during the exhumation of eclogites. The high Rb/Sr and Ba/Pb but low Pb* eclogites generally have high bulk-rock $\delta^{26}\text{Mg}$ values, whereas high Pb* and $^{87}\text{Sr}/^{86}\text{Sr}$ eclogites have mantle-like $\delta^{26}\text{Mg}$ values, suggesting diverse influences of the two fluid components on the Mg isotopic systematics of these eclogites. The LILE-rich fluid component, possibly derived from mica-group minerals, contains a considerable amount of heavy Mg that has shifted $\delta^{26}\text{Mg}$ of the eclogites towards higher values. By contrast, the $^{87}\text{Sr}/^{86}\text{Sr}$ - and Pb-rich fluid component, most likely released from epidote-group minerals in metasediments, has little Mg so as not to modify the Mg isotopic composition of the eclogites. In addition, the influence of talc-derived fluid might be evident in a very few eclogites that have low Rb/Sr and Ba/Pb but slightly heavier Mg isotopic compositions. These findings represent an important step toward a broad understanding of the Mg isotope geochemistry in subduction zones, and contributing to understanding why island arc basalts have averagely heavier Mg isotopic compositions than the normal mantle.

Highlights:

1. Tianshan eclogites were interacted with two fluid components during exhumation.
2. The high-LILEs component is likely released from mica-group minerals.
3. The high-LILEs component contains a significant amount of isotopically heavy Mg.
4. The high-Pb component is possibly dehydrated from epidote-group minerals.
5. The high-Pb component contains too little Mg so as not to influence the eclogites.

1 **Tracing subduction zone fluid-rock interactions using**
2 **trace element and Mg-Sr-Nd isotopes**

3
4 Shui-Jiong Wang^{1,2*}, Fang-Zhen Teng^{2*}, Shu-Guang Li¹, Li-Fei Zhang³, Jin-Xue Du^{1,3}, Yong-Sheng
5 He¹, Yaoling Niu^{4,5}

6
7 ¹ State Key Laboratory of Geological Processes and Mineral Resources, China University of Geosciences,
8 Beijing 100083, China

9 ² Isotope Laboratory, Department of Earth and Space Sciences, University of Washington, Seattle, WA
10 98195-1310, USA

11 ³ School of Earth Space Sciences, Peking University, Beijing, China

12 ⁴ Institute of Oceanology, Chinese Academy of Sciences, Qingdao 266071, China

13 ⁵ Department of Earth Sciences, Durham University, Durham DH1 3LE, UK

14 Abstract: 492 words

15 Text: 5139 words

16 Figure: 6

17 Table: 2

18 Revised version submitted to *Lithos* (July 29, 2017)

19

20 *Present address: Department of Earth and Atmospheric Sciences, Indiana University, Bloomington, IN 47405
21 USA.

22 Corresponding authors: sxw057@gmail.com(S.-J. Wang); fteng@u.washington.edu (F.-Z. Teng)

23 **Abstract**

24 Slab-derived fluids play a key role in mass transfer and elemental/isotopic exchanges in
25 subduction zones. The exhumation of deeply subducted crust is achieved via a subduction
26 channel where fluids from various sources are abundant, and thus the chemical/isotopic
27 compositions of these rocks could have been modified by subduction-zone fluid-rock
28 interactions. Here, we investigate the Mg isotopic systematics of eclogites from southwestern
29 Tianshan, in conjunction with major/trace element and Sr-Nd isotopes, to characterize the
30 source and nature of fluids and to decipher how fluid-rock interactions in subduction channel
31 might influence the Mg isotopic systematics of exhumed eclogites. The eclogites have high
32 LILEs (especially Ba) and Pb, high initial $^{87}\text{Sr}/^{86}\text{Sr}$ (up to 0.7117; higher than that of coeval
33 seawater), and varying Ni and Co (mostly lower than those of oceanic basalts), suggesting
34 that these eclogites have interacted with metamorphic fluids mainly released from subducted
35 sediments, with minor contributions from altered oceanic crust or altered abyssal peridotites.
36 The positive correlation between $^{87}\text{Sr}/^{86}\text{Sr}$ and Pb^* (an index of Pb enrichment; $\text{Pb}^* =$
37 $2 \cdot \text{Pb}_N / [\text{Ce}_N + \text{Pr}_N]$), and the decoupling relationships and bidirectional patterns in
38 $^{87}\text{Sr}/^{86}\text{Sr}$ -Rb/Sr, Pb^* -Rb/Sr and Pb^* -Ba/Pb spaces imply the presence of two compositionally
39 different components for the fluids: one enriched in LILEs, and the other enriched in Pb and
40 $^{87}\text{Sr}/^{86}\text{Sr}$. The systematically heavier Mg isotopic compositions ($\delta^{26}\text{Mg} = -0.37$ to $+0.26$)
41 relative to oceanic basalts (-0.25 ± 0.07) and the roughly negative correlation of $\delta^{26}\text{Mg}$ with
42 MgO for the southwestern Tianshan eclogites, cannot be explained by inheritance of Mg
43 isotopic signatures from ancient seafloor alteration or prograde metamorphism. Instead, the
44 signatures are most likely produced by fluid-rock interactions during the exhumation of

45 eclogites. The high Rb/Sr and Ba/Pb but low Pb* eclogites generally have high bulk-rock
46 $\delta^{26}\text{Mg}$ values, whereas high Pb* and $^{87}\text{Sr}/^{86}\text{Sr}$ eclogites have mantle-like $\delta^{26}\text{Mg}$ values,
47 suggesting that the two fluid components have diverse influences on the Mg isotopic
48 systematics of these eclogites. The LILE-rich fluid component, possibly derived from
49 mica-group minerals, contains a considerable amount of isotopically heavy Mg that has
50 shifted the $\delta^{26}\text{Mg}$ of the eclogites towards higher values. By contrast, the $^{87}\text{Sr}/^{86}\text{Sr}$ - and
51 Pb-rich fluid component, most likely released from epidote-group minerals in metasediments,
52 has little Mg so as not to modify the Mg isotopic composition of the eclogites. In addition,
53 the influence of talc-derived fluid might be evident in a very few eclogites that have low
54 Rb/Sr and Ba/Pb but slightly heavier Mg isotopic compositions. These findings represent an
55 important step toward a broad understanding of the Mg isotope geochemistry in subduction
56 zones, and contributing to understanding why island arc basalts have averagely heavier Mg
57 isotopic compositions than the normal mantle.

58 **Keywords:** Mg isotopes, subduction channel, fluid-rock interaction, eclogite, Tianshan

59 **1. Introduction**

60 Subduction channel is a highly reactive interface between subducting oceanic
61 lithosphere and mantle wedge, in which mass transfer as well as elemental and isotopic
62 exchanges actively occur (*e.g.*, Bebout and Penniston-Dorland, 2016). In this region, fluids
63 released from various subducting slab lithologies (*e.g.*, sediments, altered oceanic crust, and
64 altered abyssal peridotites) can be mixed and penetrate into exhuming rocks, inducing
65 extensive fluid-rock interactions (Zack and John, 2007; John et al., 2008; van der Straaten et
66 al., 2008, 2012). The fluids, when emanating from the interface into the mantle wedge, can
67 further impart their chemical/isotopic signatures to the juxtaposed mantle rocks and
68 associated arc volcanism.

69 Trace elements in conjunction with Sr-Nd-O isotopic systematics have been widely used
70 to identify and understand fluid-rock interactions in subduction channels (Glodny et al., 2003;
71 John et al., 2004, 2012; King et al., 2006; Halama et al., 2011). The magnesium (Mg)
72 isotopic systematics might be a useful tracer of subduction-zone fluid-rock interactions,
73 potentially providing insights into the source and nature of fluids. Magnesium is fluid-mobile
74 at low temperatures, which leads to large Mg isotope fractionations as much as 7 ‰ during
75 Earth's surface processes (Teng, 2017 and references therein). Recent studies also
76 documented high mobility of Mg during subduction-zone metamorphism (van der Straaten et
77 al., 2008; Horodyskyj et al., 2009; Pogge von Strandmann et al., 2015; Chen et al., 2016).
78 Chen et al. (2016) found high $\delta^{26}\text{Mg}$ values (up to +0.72) for white schists from Western
79 Alps, and linked them to infiltration of Mg-rich fluids derived from dehydration of

80 serpentinites. Recent studies also documented generally heavier Mg isotopic compositions in
81 arc volcanic rocks relative to normal peridotitic sources ($\delta^{26}\text{Mg} = -0.25 \pm 0.07$), which were
82 explained as the addition of heavy Mg isotopes from subducting slabs to the mantle wedge
83 (Teng et al., 2016; Li et al., 2017). A general conclusion derived from these studies is that the
84 subduction-zone fluids might be isotopically heavy in terms of Mg isotopes. Nevertheless,
85 the interpretation of any Mg isotopic variations in subduction-related rocks requires the
86 knowledge of how Mg isotopes behave in subduction channels, and how fluid-rock
87 interactions could affect the Mg isotopic systematics of a rock.

88 Orogenic eclogites of seafloor protolith may be the best choice to study subduction
89 channel processes. Oceanic crust undergoes seawater alteration prior to subduction and is,
90 therefore, more hydrated relative to the continental crust (Miller et al., 1988). It experiences
91 extensive dehydration together with the sediment veneer during subduction (Gerya et al.,
92 2002). In addition, the exhumation of oceanic crust via the subduction channel proceeds at
93 relatively slower rate (mm/yr; Agard et al., 2009). All of these allow eclogites of seafloor
94 protolith to preserve a record of extensive fluid-rock interactions during exhumation. An
95 increasing number of studies have shown that fluid-rock interactions can readily modify the
96 chemical and isotopic compositions of exhumed eclogites (*e.g.*, Bebout, 2007; Xiao et al.,
97 2012; Klemd, 2013), although how the chemical/isotopic composition shift depends on the
98 nature and abundance of fluids with which the eclogites have interacted.

99 In this study, we investigate a suite of well-characterized eclogites/blueschists and mica
100 schists from southwestern Tianshan, China. We present the first Mg isotopic data for the

101 orogenic eclogites of seafloor protolith, and in combination with Sr-Nd isotopic and trace
102 elemental data, we explore the influence of subduction-zone fluid-rock interactions on the
103 Mg isotopic systematics of eclogites. Our results show that these eclogites are variably
104 enriched in heavy Mg isotopes, which may result from interactions of the eclogites with both
105 high-MgO and low-MgO fluids released from different hydrous minerals in the subduction
106 channel.

107 **2. Geological settings and samples**

108 The high-pressure to ultrahigh-pressure (HP-UHP) metamorphic belt of Chinese
109 southwestern Tianshan, located along the suture between the Yili and the Tarim blocks, was
110 formed during the northward subduction of the Palaeo-South Tianshan oceanic crust beneath
111 the Yili block (Windley et al., 1990; Gao et al., 1999; Zhang et al., 2002, 2008). The eclogites
112 and retrograded blueschists in southwestern Tianshan occur as interlayers or lenticular bodies
113 in mica schists, representing the relic oceanic crust that experienced subduction and
114 exhumation in response to later continental collision. The protoliths of eclogites and
115 associated blueschists range from MORBs to OIBs as indicated by the geochemical data and
116 their preserved pillow structures in the field (Zhang et al., 2002, 2008; Gao and Klemd, 2003;
117 Ai et al., 2006). The eclogites and their host rocks have experienced peak coesite-bearing
118 eclogite-facies metamorphism at 324 ~ 312 Ma (Zhang et al., 2005; Su et al., 2010; Klemd et
119 al., 2011; Li et al., 2011a; Yang et al., 2013), followed by a slow exhumation rate to
120 amphibolite-facies between 320 Ma and 240 Ma (*e.g.*, Zhang et al., 2013). The peak and
121 retrograde metamorphic temperatures estimated for the southwestern Tianshan eclogites vary

122 from 450 to 630 °C (*e.g.*, Du et al., 2014a, b). The retrograde metamorphic temperatures are
123 slightly higher than the peak-eclogite facies temperatures as a result of thermal relaxation
124 during the exhumation (*e.g.*, Zhang et al., 2013). The presence of abundant millimeter to
125 decimeter-wide and centimeter to meter-long veins in southwestern Tianshan blueschists and
126 eclogites indicates extensive fluid-rock interactions and fluid-mediated mass transport during
127 crustal subduction and exhumation (Gao and Klemd, 2001; Gao et al., 2007; John et al., 2008;
128 2012; Beinlich et al., 2010; Lü et al., 2012).

129 The petrology and metamorphic evolution of the studied eclogites and mica schists have
130 been well characterized (Zhang et al., 2003; Ai et al., 2006; Lü et al., 2009; Du et al., 2011,
131 2014b; Xiao et al., 2012). The eclogites consist mainly of garnet, omphacite, glaucophane,
132 paragonite, epidote, calcite, dolomite and quartz/coesite; the mica schists are mainly
133 composed of garnet, glaucophane, phengite, epidote, paragonite, plagioclase and
134 quartz/coesite. A detail description of the studied eclogites and mica schists including the
135 sample localities has been given in Supplementary Table S1.

136 **3. Analytical methods**

137 **3.1 Major and trace elements**

138 Major elements were analyzed at the Hebei Institute of Regional Geology and Mineral
139 Resources, China, by wavelength dispersive X-Ray fluorescence spectrometry (Gao et al.,
140 1995). Analytical uncertainties are generally better than 1%. The H₂O⁺ and CO₂ were
141 determined by gravimetric methods and potentiometry, respectively. Trace elements were
142 analyzed using an Elan 6100 DRC ICP-MS at the CAS key laboratory of crust-material and

143 environments, University of Science and Technology of China, Hefei. Samples were
144 analyzed with aliquots of USGS whole-rock standards BHVO-2, BIR-1, AGV-2 and GSP-2,
145 which were treated as unknown. Results for the USGS standards together with the reference
146 values are reported in Supplementary Table S2. Analytical uncertainties are better than 5%
147 for most of the elements.

148 **3.2 Strontium and Nd isotopic analysis**

149 The Sr and Nd were separated from the matrix with cation exchange chromatography
150 with Bio-Rad AG50W-X12 resin using the method described by Chu et al. (2009). The Sr
151 and Nd isotopes were performed using an Isoprobe-T thermal ionization mass spectrometer
152 (TIMS) at the State Key Laboratory of Lithospheric Evolution, Institute of Geology and
153 Geophysics, Chinese Academy of Sciences. Measured $^{87}\text{Sr}/^{86}\text{Sr}$ and $^{143}\text{Nd}/^{144}\text{Nd}$ ratios were
154 corrected for mass-fractionation using $^{86}\text{Sr}/^{88}\text{Sr} = 0.1194$ and $^{146}\text{Nd}/^{144}\text{Nd} = 0.7219$,
155 respectively. During the course of this study, standards of NBS987-Sr and jNdi-Nd give a
156 value of $^{87}\text{Sr}/^{86}\text{Sr} = 0.710245 \pm 20$ and $^{143}\text{Nd}/^{144}\text{Nd} = 0.512117 \pm 10$, respectively.

157 **3.3 Magnesium isotopic analysis**

158 Magnesium isotopic ratios were analyzed for bulk rock powders and mineral separates
159 at the University of Washington, Seattle. The separation of Mg was achieved by cation
160 exchange chromatography using Bio-Rad AG50W-X8 resin in 1N HNO₃ media (Teng et al.,
161 2007, 2010a; 2015; Yang et al., 2009; Li et al., 2010). Two standards, Kilbourne Hole (KH)
162 olivine and seawater, were processed together with samples for each batch of column
163 chemistry. The Mg isotopic ratios were determined using the standard-sample bracketing

164 protocol on a *Nu* plasma MC-ICPMS (Teng and Yang, 2014). The blank Mg signal for ^{24}Mg
165 was $< 10^{-4}$ V, which is negligible relative to the sample signals of 3-5 V. The KH olivine and
166 seawater yielded average $\delta^{26}\text{Mg}$ of -0.25 ± 0.05 and -0.82 ± 0.06 , respectively, consistent
167 with previous reported values (Foster et al., 2010; Li et al., 2010; Teng et al., 2010; Ling et
168 al., 2011; Wang et al., 2016)

169 **4. Results**

170 Major and trace elemental compositions of the eclogites and mica schists are
171 summarized in Supplementary Table S3. The eclogites have SiO_2 ranging from 39.82 to
172 52.47 wt.% and MgO ranging from 3.19 to 9.68 wt.% (Supplementary Table S3), and plot in
173 subalkalic basalt field in Zr/Ti versus Nb/Y diagram (Supplementary Fig. S1; Pearce, 1996).
174 The high contents of H_2O^+ (0.58 to 3.38 wt.%) and CO_2 (0.08 to 8.96 wt.%) are consistent
175 with the presence of water- and/or carbon oxide-bearing minerals such as zoisite/clinozoisite
176 and calcite/dolomite. The eclogites have variably high LILEs (*e.g.*, Ba, Rb, Cs, and K) and
177 Pb, but low Ni and Co concentrations (Supplementary Table S3). The mica schists are felsic
178 with SiO_2 ranging from 59.53 to 76.66 wt.% and MgO ranging from 1.81 to 3.60 wt.%
179 (Supplementary Table S3). They are characterized by variable contents of LILEs, Sr and Pb,
180 which may be controlled by different proportions of mica-group minerals (host of LILEs) and
181 epidote-group minerals (major host of Sr and Pb) in southwestern Tianshan metasediments
182 (*e.g.*, Xiao et al., 2012).

183 The Sr and Nd isotopic compositions of the eclogites are reported in Table 1. The
184 eclogites have positive age-corrected $\epsilon\text{Nd}_{320\text{Ma}}$ value ranging from +2.8 to +10.1 (with one

185 exception of -2.4; Fig. 1). They have extremely high and variable initial Sr isotopic
186 compositions ($^{87}\text{Sr}/^{86}\text{Sr}_{320\text{Ma}}$) varying from 0.7058 to 0.7117 (Fig. 1), a range that is even
187 higher than that of Ordovician to Carboniferous seawater ($^{87}\text{Sr}/^{86}\text{Sr} = 0.7075 - 0.7090$; Veizer,
188 1989). As a result, the eclogites plot rightward far from the field defined by depleted MORB
189 and OIB in $\epsilon\text{Nd}(t) - ^{87}\text{Sr}/^{86}\text{Sr}(t)$ diagram (Fig. 1).

190 The $\delta^{26}\text{Mg}$ values of southwestern Tianshan eclogites vary widely from -0.37 ± 0.05 to
191 $+0.26 \pm 0.04$ (Table 2), equal to or higher than unaltered oceanic basalts and eclogites of
192 continental basalt protolith, both of which have homogeneous Mg isotopic compositions
193 around the normal mantle value (-0.25 ± 0.07 ; Fig. 2). Garnets in southwestern Tianshan
194 eclogites yield $\delta^{26}\text{Mg}$ values varying from -1.75 ± 0.07 to -1.10 ± 0.07 , and omphacites have
195 $\delta^{26}\text{Mg}$ values ranging from -0.04 ± 0.05 to $+0.46 \pm 0.07$ (Table 2), with corresponding
196 inter-mineral Mg isotope fractionation ($\Delta^{26}\text{Mg}_{\text{Cpx-Grt}} = \delta^{26}\text{Mg}_{\text{Cpx}} - \delta^{26}\text{Mg}_{\text{Grt}}$) in the range of
197 1.23 - 1.98. Temperatures estimated using garnet-clinopyroxene Mg isotope geothermometer
198 range from 485°C to 675°C (Huang et al., 2013; Li et al., 2016b) , which are in rough
199 agreement with the peak and retrograde metamorphic temperatures for the Tianshan eclogites
200 (*e.g.*, Du et al., 2014a, b). Six mica schists from southwestern Tianshan have bulk $\delta^{26}\text{Mg}$
201 values ranging from -0.11 ± 0.05 to $+0.23 \pm 0.02$ (Table 2).

202 **5. Discussion**

203 The overprint of fluid-rock interactions on the southwestern Tianshan
204 eclogites/blueschists has been confirmed by many petrological and geochemical studies (John
205 et al., 2008; van der Straaten et al., 2008, 2012; Beinlich et al., 2010; Lü et al., 2012; Li et al.,

206 2016a; Zhang et al., 2016). Depending on the nature and abundance of fluids in a subduction
207 channel, the initial composition of an eclogite can be altered to various degrees after
208 fluid-rock interactions. In this section, we first focus on the trace element and Sr-Nd isotopes
209 to characterize the source and nature of the fluids, and then decipher how fluid-rock
210 interactions may have influenced the Mg isotopic systematics of the eclogites. Finally, we
211 discuss the Mg isotope geochemistry of slab-derived fluids in the subduction channel and
212 their influences on the sub-arc peridotites.

213 **5.1 Geochemical evidence for fluid-rock interactions**

214 Trace element and Sr-Nd isotope geochemistry suggest interactions of eclogites with
215 metamorphic fluids. The fluids are mainly derived from subducted sediments, with limited
216 contributions from serpentinites or altered oceanic crusts. Most eclogites are variably
217 enriched in LILEs (*e.g.*, Ba, Cs, Rb, and K) and Pb (Fig. 3), which can be produced during
218 either ancient seafloor alteration or subduction-zone fluid-rock interactions. Bebout (2007)
219 documented that significant enrichments of Ba and Pb in metabasaltic rocks can be most
220 directly associated with metasomatism because these two elements are only slightly enriched
221 in altered oceanic basalts during seafloor alteration relative to other LILEs. The consistently
222 high Ba/Rb, high Ba/K and low Ce/Pb of our eclogites are thus indicative of HP/UHP
223 fluid-rock interactions rather than ancient seawater alteration (Fig. 3a, b, c). Furthermore,
224 these eclogites have extremely high initial $^{87}\text{Sr}/^{86}\text{Sr}$ ratio up to 0.7117 (Fig. 1), a signature
225 that cannot be attributed to pre-subduction seawater alteration because the
226 Ordovician-Carboniferous seawater has much lower $^{87}\text{Sr}/^{86}\text{Sr}$ ratios of 0.7075 - 0.7090

227 (Veizer, 1989). The high $^{87}\text{Sr}/^{86}\text{Sr}_{320\text{Ma}}$ ratios thus must have resulted from interactions of the
228 eclogites with fluids during metasomatism, and the fluids might be derived from subducted
229 sediments whose $^{87}\text{Sr}/^{86}\text{Sr}$ ratios can be as high as 0.73 (Plank and Langmuir, 1998). In
230 contrast to Sr isotopes, Nd isotopes appear to behave conservatively during the metasomatism
231 (King et al., 2006). Due to the low mobility of REE during metamorphic dehydration under
232 relatively low P-T conditions (Kessel et al., 2005), slab-derived fluids would contain too little
233 Nd to affect the Nd isotopic systematics of eclogites (van der Straaten et al., 2012), such that
234 the eclogites retain their depleted Nd isotopic signatures (Fig. 1). In accordance with the high
235 $^{87}\text{Sr}/^{86}\text{Sr}$ ratios, most eclogites contain very low concentrations of Co and Ni evolving from
236 oceanic basalts towards the GLOSS (global subducting sediments; Fig. 3d), pointing towards
237 again interactions of the eclogites with sediment-derived fluids. Some eclogites however
238 have Ni and Co contents overlapping or slightly higher than oceanic basalts (Fig. 3d). This
239 indicates the possible contributions of altered oceanic crust-derived or serpentinite-derived
240 fluids (*e.g.*, van der Straaten et al., 2012), although subducted sediments must be the
241 dominant source for fluids that have interacted with the eclogites.

242 The geochemical signatures of sediment-derived fluids might vary significantly in
243 response to the mineralogical heterogeneity of subducting sediments. The eclogites display a
244 series of geochemical features indicative of two compositionally different fluid components
245 (Fig. 4). As shown in Rb/Sr vs. Pb^* (an index of enrichment of Pb; $\text{Pb}^* = 2 \cdot \text{Pb}_\text{N} / [\text{Ce}_\text{N} + \text{Pr}_\text{N}]$)
246 and Ba/Pb vs. Pb^* diagrams, the enrichment of Pb in eclogites is not always associated with
247 the enrichment of LILEs (Fig. 4a and b). The observed decoupling patterns may indicate two
248 major fluid components: one enriched in LILEs relative to Pb (*e.g.*, high Rb/Sr and Ba/Pb but

249 low Pb*), and the other enriched in Pb relative to LILEs (*e.g.*, high Pb* but low Rb/Sr or
250 Ba/Pb). The roughly positive correlation between Pb* and $^{87}\text{Sr}/^{86}\text{Sr}_{320\text{Ma}}$ (Fig. 4c), suggests
251 that the high-Pb component also contains a significant amount of radiogenic Sr that has
252 elevated the $^{87}\text{Sr}/^{86}\text{Sr}$ value of eclogites. Some carbonated eclogites are extremely enriched in
253 elemental Sr but have relatively low $^{87}\text{Sr}/^{86}\text{Sr}$ values of 0.7066 – 0.7078 (Supplementary Fig.
254 S2), suggesting that the surrounding marbles are not the source of high- $^{87}\text{Sr}/^{86}\text{Sr}$ fluid. Instead,
255 the high- $^{87}\text{Sr}/^{86}\text{Sr}$ fluid component must be sourced from other metasediments, such as mica
256 schists. The high-LILEs component, on the other hand, might contain too little Sr to modify
257 the Sr isotopic composition of eclogites, as reflected by the decoupling relationship between
258 $^{87}\text{Sr}/^{86}\text{Sr}_{320\text{Ma}}$ and Rb/Sr (Fig. 4d): the high-Rb/Sr eclogites display low $^{87}\text{Sr}/^{86}\text{Sr}_{320\text{Ma}}$ values,
259 whereas the low-Rb/Sr samples are characterized by highly radiogenic Sr isotopic
260 compositions (Fig. 4d). All these observations support that the eclogites were infiltrated by
261 two fluid components. The distinct geochemical signatures of the two fluid components are
262 consistent with the fact that LILEs and Sr-Pb are hosted in different hydrous minerals in
263 subducted sediments: mica-group minerals are the dominant host for LILEs, whereas
264 epidote-group minerals (and to a less extent carbonate minerals and paragonite) are the major
265 host of Pb and Sr (*e.g.*, Busigny et al., 2003; Bebout et al., 2007, 2013; Xiao et al., 2012). As
266 a result, fluid dehydrated from mica-group minerals would have high Rb/Sr and Ba/Pb ratios,
267 whereas fluid released from epidote-group minerals in metasediments could be enriched in
268 Pb and Sr (as well as $^{87}\text{Sr}/^{86}\text{Sr}$). It is possible that varying modal mineralogy in the subducted
269 sediments (*e.g.*, mica-group minerals are abundant in metapelites and epidote-group minerals
270 are abundant in greywackes) can result in decomposition of mica- and epidote-group

271 minerals in different proportions along the subduction P-T path and generate the two fluid
272 components in the subduction channel. During crustal subduction, biotite is thought to be
273 completely decomposed at $P = 1.3-1.5$ GPa, at which the epidote-group minerals such as
274 epidote and zoisite are still stable (Poli and Schmidt, 2002). Therefore, decomposition of
275 biotite at the early stage during crustal subduction could release a significant amount of fluid
276 that is enriched in LILEs. At a higher pressure above 2.5 GPa, epidote and zoisite might
277 become unstable (Carswell, 1990; Poli and Schmidt, 2002). Metamorphic dehydration at this
278 stage could thus release abundant Sr and Pb to the fluids. Such fluids, when released from
279 subducting oceanic crust, would migrate upward along the subduction channel, infiltrate the
280 exhuming eclogites and impart their distinct geochemical signatures to the eclogites via
281 fluid-rock interactions.

282 **5.2 Constraining the mechanisms of Mg isotopic variations in the eclogites**

283 The eclogites have varying Mg contents ($MgO = 3.2$ to 9.7 wt.%) at a given SiO_2
284 content, and more variable and systemically heavier Mg isotopic composition than fresh
285 oceanic basalts (Fig. 5). The simplest explanation for the low MgO and high $\delta^{26}Mg$ of
286 eclogites is physical/mechanical mixing with a high- $\delta^{26}Mg$ sedimentary component at some
287 point before or during the exhumation of the eclogites. However, this is very unlikely
288 because binary mixing calculation, using the highest $\delta^{26}Mg$ value of the six mica schists as an
289 endmember (Q-314), suggests that at least $>60\%$ of sedimentary component is required to
290 produce the Mg isotopic compositions of most eclogites (Fig. 5), such that the eclogites
291 would have anomalously high SiO_2 contents (>55 wt.%). In addition, the SiO_2 of eclogites

292 does not correlate with neither $^{87}\text{Sr}/^{86}\text{Sr}_{320\text{Ma}}$ nor $\epsilon\text{Nd}(t)$ (Supplementary Fig. S3), further
293 supporting that binary mixing between basalt (or eclogite) and sediment (or metasediment)
294 might not be the case. Magnesium is fluid-mobile, thus, processes like ancient seawater
295 alteration, prograde metamorphism (*e.g.*, release of Mg into metamorphic fluids and
296 eclogite-host isotopic exchanges), and retrograde fluid-rock interactions (*e.g.*, interaction
297 with metamorphic fluid during exhumation), could potentially account for the observed Mg
298 isotopic variations. Next, we endeavor to explore how Mg isotopes behave during these
299 processes, based on which, we highlight the importance of subduction channel fluids in
300 generating Mg isotopic variations in exhumed eclogites.

301 *5.2.1 Seafloor alteration cannot explain the Mg isotopic signatures*

302 Seafloor alteration produces even larger Mg isotopic variations, with Mg isotopes likely
303 fractionated in a different manner from that observed in the eclogites, as shown in Fig. 5.
304 Altered oceanic crusts (AOC) from two different sites have been reported for Mg isotopic
305 compositions (Huang et al., 2015; Teng, 2017). Carbonate-barren AOC samples recovered
306 from IODP site 1256 in the eastern equatorial Pacific retain a mantle-like $\delta^{26}\text{Mg}$ value as for
307 fresh oceanic basalts (Fig. 5; Huang et al., 2015), based on which Huang et al. (2015)
308 concluded that seafloor alteration causes limited Mg isotope fractionation, regardless of
309 alteration temperature and water/rock ratio. At the other site (ODP site 801) in western
310 Pacific, extensively altered AOC samples have highly variable $\delta^{26}\text{Mg}$ values ranging from
311 -2.76 to +0.21 (Fig. 5), with low $\delta^{26}\text{Mg}$ values being associated with carbonate enriched
312 samples and high $\delta^{26}\text{Mg}$ values associated with clay-rich samples (Teng, 2017). Due to

313 carbonate dilution effect (Tipper et al., 2006), the AOC samples from ODP site 801 are
314 distributed in a trend in which $\delta^{26}\text{Mg}$ values decrease as MgO decreases (Fig. 5). Different
315 from AOC, none of the studied eclogites (32 in total) show enrichment of light Mg isotopes,
316 although they contain variable abundances of carbonate minerals. Furthermore, neither
317 heavily nor less altered AOC could account for the roughly negative correlation between
318 $\delta^{26}\text{Mg}$ and MgO for the eclogites (Fig. 5). Thus, ancient seawater alteration is unlikely to be
319 the cause of the variable and systemically heavier Mg isotopic compositions of the eclogites.

320 *5.2.2 The role of prograde metamorphic dehydration and eclogite-host isotopic exchange*

321 Magnesium isotope fractionation during prograde metamorphic dehydration or
322 eclogite-host isotopic exchange cannot account for the Mg isotopic variations in our eclogites.
323 It is possible that dehydrated fluids have distinct Mg isotopic compositions from the rock
324 where the fluids are from. However, since the fraction of Mg partitioning into the fluid
325 phases is so small compared to that inherited by metamorphic minerals during prograde
326 metamorphism, metamorphic dehydration causes insignificant Mg isotope fractionation ($<$
327 ± 0.07) on a bulk-rock scale (Li et al., 2011b, 2014; Teng et al., 2013; Wang et al., 2014b,
328 2015a, b). Local isotopic exchange between eclogite and its host rock can potentially change
329 the original mantle-like Mg isotopic compositions of the eclogites (Wang et al., 2014a). To
330 which direction the Mg isotopes of the eclogites fractionate depends on the types of host rock.
331 For example, eclogite-host isotopic exchange would make eclogite boudins in
332 carbonates/marbles isotopically lighter, whereas those enclosed in mica schists heavier
333 (Wang et al., 2014a). However, no systemic relationship between $\delta^{26}\text{Mg}$ and host rock type

334 was observed for the southwestern Tianshan eclogites. On the opposite, the carbonated
335 eclogites (those enclosed in marbles) in our study are enriched in heavy Mg isotopes ($\delta^{26}\text{Mg}$
336 = -0.28 to +0.02; Table 2), which we interpret below as a result of infiltration of external
337 fluids derived from metasediments.

338 *5.2.3 Response of Mg isotopic systematics in the eclogites to fluid-rock interactions.*

339 Thus, our favored interpretation of the Mg isotopic variation is fluid-rock interaction in
340 a subduction channel. The fluids must be enriched in heavy Mg isotopes, and pervasively
341 reactive in interacting with the eclogites because the eclogites have systemically heavier Mg
342 isotopic compositions (Fig. 2), regardless of their diverse host rock types. Below, we discuss
343 how the two fluid components may have affected the Mg isotopic compositions of the
344 eclogites.

345 The two fluid components, due to their derivation from different hydrous minerals,
346 have different impacts on the Mg isotopic systematics of eclogites. In the plots of $\delta^{26}\text{Mg}$ vs.
347 Pb^* and $\delta^{26}\text{Mg}$ vs. $^{87}\text{Sr}/^{86}\text{Sr}_{320\text{Ma}}$ (Fig. 6a and b), the high- Pb^* and $^{87}\text{Sr}/^{86}\text{Sr}_{320\text{Ma}}$ samples
348 retain a mantle-like $\delta^{26}\text{Mg}$ value, suggesting that the infiltration of high-Pb and $^{87}\text{Sr}/^{86}\text{Sr}$ fluid
349 component had limited influences on the Mg isotopic composition of eclogites. Being the
350 dominant source of high-Pb and $^{87}\text{Sr}/^{86}\text{Sr}$ component, the epidote-group minerals contain
351 little Mg (*e.g.*, Guo et al., 2012), and thus the fluid dehydrated from them is unable to modify
352 the Mg isotopic composition of the eclogites (although the exact $\delta^{26}\text{Mg}$ value of any
353 epidote-group mineral has not been reported so far). The low- Pb^* and $^{87}\text{Sr}/^{86}\text{Sr}_{320\text{Ma}}$ samples,
354 on the other hand, have variably high $\delta^{26}\text{Mg}$ values (Fig. 6a and b). As expected, eclogites

355 with high-Rb/Sr and Ba/Pb ratios have high $\delta^{26}\text{Mg}$ values (Fig. 6c and d). Because of the
356 complexity of the fluid system and the uncertainty of its Mg concentration and Mg isotopic
357 composition, we are not expecting to see good correlations between $\delta^{26}\text{Mg}$ and indices of
358 enrichment of LILEs (such as Rb/Sr and Ba/Pb). However, the general patterns shown in Fig.
359 6c and d suggest that the high-LILEs component carries a significant amount of isotopically
360 heavy Mg that has elevated the $\delta^{26}\text{Mg}$ values of the eclogites. Mica-group minerals, as the
361 major source of high-LILE component, are enriched in MgO, and in addition their $\delta^{26}\text{Mg}$
362 values are characteristically high. For instance, biotites in metapelites from the Ivrea Zone in
363 NW Italy have $\delta^{26}\text{Mg}$ values ranging from -0.08 to +1.10 (Wang et al., 2015b), and phengites
364 in eclogites from the Dabie orogen have $\delta^{26}\text{Mg}$ values of +0.30 to +0.59 (Li et al., 2011b).
365 Therefore, eclogites metasomatized by the mica-derived fluid could gain high- $\delta^{26}\text{Mg}$
366 signatures. It is also important to note that in Fig. 6c and d, a part of low-Rb/Sr and Ba/Pb
367 samples has slightly high $\delta^{26}\text{Mg}$ value, which we interpret as the possible influence of the
368 talc-derived fluid, as the talc in serpentinite is depleted in LILEs but enriched in heavy Mg
369 ($\delta^{26}\text{Mg} = +0.06$ to +0.30; Beinlich et al., 2014). Without good constraints on the Mg isotopic
370 composition of fluid and the partition coefficient of MgO between fluid and eclogite, it is not
371 yet possible to give a perfect fluid-rock interaction model for the whole dataset of the
372 eclogites. However, the rough negative correlation between $\delta^{26}\text{Mg}$ and MgO for the eclogites
373 can be generally modeled as interactions of eclogites with high-MgO (*e.g.*, dehydrated from
374 mica-group minerals or talc) and low-MgO fluid components (*e.g.*, dehydrated from
375 epidote-group minerals) under a variety of water/rock (fluid/eclogite) ratios (Fig. 5).

376 **5.3 The origins of isotopically heavy fluids in subduction channel**

377 Fluids in subduction channels are likely to have heavy Mg isotopic compositions,
378 although different subducted lithologies themselves show highly variable $\delta^{26}\text{Mg}$ values. The
379 subducted abyssal peridotites have slightly high $\delta^{26}\text{Mg}$ values of -0.25 - +0.10 (Liu et al.,
380 2017). The subducted sediments and altered oceanic crusts have large variations in $\delta^{26}\text{Mg}$
381 values (-2.76 ‰ to +0.92 ‰), with low $\delta^{26}\text{Mg}$ associated with carbonated rocks and with
382 high $\delta^{26}\text{Mg}$ associated with carbonate-free rocks (Li et al., 2010; Wang et al., 2015a; Huang
383 et al., 2015; Teng et al., 2016; Hu et al., 2017; Teng, 2017). One might expect that subsolidus
384 decarbonation or carbonate dissolution during metamorphism could release light Mg isotopes,
385 making the sediment-derived fluids isotopically light. However, decarbonation is an
386 inefficient process for carbonated sediments/basalts along the P-T paths of oceanic
387 subduction (Gorman et al., 2006; Dasgupta and Hirschmann, 2010). Carbonate species
388 dissolved in metamorphic fluid is thought to be mainly CaCO_3 (Ague and Nicolescu, 2014;
389 Kelemen and Manning, 2015; Li et al., 2017). Therefore, the presence of carbonate minerals
390 in subducted rocks has negligible influence on the Mg isotopic composition of dehydrated
391 fluids (Li et al., 2017). By contrast, breakdown of hydrous minerals might control the Mg
392 concentration and Mg isotopic composition of dehydrated fluids. Reported $\delta^{26}\text{Mg}$ values for
393 Mg-rich hydrous minerals, such like mica-group minerals and talc, are higher than the normal
394 mantle value (Li et al., 2011b; Beinlich et al., 2014; Wang et al., 2015b), and thus it is very
395 likely that the dehydrated fluids are enriched in heavy Mg isotopes. For example, a recent
396 study suggested that the fluid derived from talc and antigorite in serpentinite is likely
397 characterized by high-Mg and high- $\delta^{26}\text{Mg}$, and could be responsible for the high $\delta^{26}\text{Mg}$
398 values of white schists in Western Alps (Chen et al., 2016).

399 **5.4 Implications on Mg isotopic systematics in sub-arc peridotites**

400 Fluids in subduction channels can infiltrate the mantle wedge, inducing fluid-peridotite
401 interactions and potentially modifying the Mg isotopic composition of associated peridotites.
402 Only a few Mg isotopic data have been reported so far for mantle wedge peridotites, and they
403 are indeed enriched in heavy Mg isotopes: six arc peridotites from Avacha Volcano in
404 Kamchatka analyzed by Pogge von Strandmann et al. (2011) have $\delta^{26}\text{Mg}$ values ranging from
405 -0.25 to -0.06, higher than the normal mantle value (-0.25 ± 0.07 ; Teng et al., 2010).
406 Although the actual mechanism responsible for the Mg isotopic variations in these peridotites
407 is still uncertain, their high $\delta^{26}\text{Mg}$ values are consistent with petrological and geochemical
408 evidence suggesting that these peridotites have been affected by upward fluid migration from
409 the subducting slab (Ionov and Seitz, 2008). Most recently, Li et al. (2017) found that island
410 arc or back arc basin basalts from circum-Pacific arcs, including Kamchatka, Philippines,
411 Costa Rica and Lau Basin have generally high $\delta^{26}\text{Mg}$ values ranging from -0.35 to +0.06.
412 Teng et al. (2016) reported the Martinique arc lava $\delta^{26}\text{Mg}$ values of -0.25 to -0.10. Those
413 values overlap the Avacha peridotites and are systemically higher than normal oceanic
414 basalts and peridotites, consistent with the interpretation that isotopically heavy fluids
415 released from the subducted slab incorporate into the mantle wedge (Teng et al., 2016; Li et
416 al., 2017). All the three cases suggest that massive flux of dehydrated fluid into the sub-arc
417 mantle could facilitate extensive fluid-peridotite interaction and shift the $\delta^{26}\text{Mg}$ of sub-arc
418 peridotite towards higher values.

419 **6. Conclusions**

420 To reveal the nature of fluid-rock interactions in subduction channels and the influence
421 of subduction-zone fluids on the Mg isotopic systematics in exhumed rocks, we present
422 major and trace elements, and Sr-Nd-Mg isotopic data for the eclogites and mica schists from
423 southwestern Tianshan, China. The following conclusions can be drawn:

424 (1) The eclogites have high Ba/Rb and Ba/K but low Ce/Pb ratios, suggesting the
425 overprint of subduction-zone metamorphic metasomatism. The highly radiogenic Sr
426 isotopic composition ($^{87}\text{Sr}/^{86}\text{Sr}_{320\text{Ma}} = 0.7058\text{-}0.7117$; higher than that of coeval
427 seawater), together with the varying and mostly low Ni and Co concentrations,
428 further indicate that the eclogites have interacted with fluids mainly released from
429 subducted sediments, with limited contributions from altered oceanic crust- or
430 serpentinite-derived fluids.

431 (2) The positive correlation between $^{87}\text{Sr}/^{86}\text{Sr}$ and Pb^* , and the bidirectional patterns in
432 $^{87}\text{Sr}/^{86}\text{Sr} - \text{Rb}/\text{Sr}$, $\text{Pb}^* - \text{Rb}/\text{Sr}$, and $\text{Pb}^* - \text{Ba}/\text{Pb}$ spaces, suggest interaction of the
433 eclogites with compositionally different two fluid components: the high-LILEs
434 component which could be derived from dehydration of mica-group minerals, and
435 the high-Pb and $^{87}\text{Sr}/^{86}\text{Sr}$ component likely released from epidote-group minerals in
436 subducted sediments.

437 (3) The highly variable and systemically heavy Mg isotopic compositions of eclogites
438 ($\delta^{26}\text{Mg} = -0.37$ to $+0.26$ ‰) resulted from fluid-rock interactions in the subduction
439 channel. The high-LILE component, dehydrated from Mg-rich mica-group minerals
440 or to a less extent from talc, contains a considerable amount of Mg that has shifted
441 the $\delta^{26}\text{Mg}$ of the eclogites towards higher values. The high-Pb and $^{87}\text{Sr}/^{86}\text{Sr}$

442 component, dehydrated from Mg-poor epidote-group minerals, has little Mg so as
443 not to influence the Mg isotopic composition of the eclogites.

444 **Acknowledgement**

445 The authors would like to thank two anonymous reviewers for insightful comments and
446 Editor Sun-Lin Chung for careful and efficient handling. This study was financially
447 supported by National Natural Science Foundation of China (41230209) to SGL, National
448 Science Foundation (EAR-1340160) to FZT, and National Science Foundation of China
449 (Grants 41330210, 41520104004) and Major State Basic Research Development Program
450 (Grant 2015CB856105) to LFZ.

451 **Reference**

- 452 Agard, P., Yamato, P., Jolivet, L. and Burov, E. (2009) Exhumation of oceanic blueschists
453 and eclogites in subduction zones: timing and mechanisms. *Earth-Science Reviews* 92,
454 53-79.
- 455 Ague, J.J. and Nicolescu, S. (2014) Carbon dioxide released from subduction zones by
456 fluid-mediated reactions. *Nature Geoscience* 7, 355-360.
- 457 Ai, Y.L., Zhang, L.F., Li, X.P., Qu, J.F., (2006) Geochemical characteristics and tectonic
458 implications of HP-UHP eclogites and blueschists in southwestern Tianshan, China. *Progress*
459 *in Natural Science* 16, 624-632.
- 460 Bebout, G.E. (2007) Metamorphic chemical geodynamics of subduction zones. *Earth and*
461 *Planetary Science Letters* 260, 373-393.
- 462 Bebout, G.E., Agard, P., Kobayashi, K., Moriguti, T. and Nakamura, E. (2013)
463 Devolatilization history and trace element mobility in deeply subducted sedimentary rocks:
464 Evidence from Western Alps HP/UHP suites. *Chemical Geology* 342, 1-20.
- 465 Bebout, G.E., Bebout, A.E. and Graham, C.M. (2007) Cycling of B, Li, and LILE (K, Cs, Rb,
466 Ba, Sr) into subduction zones: SIMS evidence from micas in high-P/T metasedimentary
467 rocks. *Chemical Geology* 239, 284-304.
- 468 Bebout, G.E. and Penniston-Dorland, S.C. (2016) Fluid and mass transfer at subduction
469 interfaces—The field metamorphic record. *Lithos* 240–243, 228-258.

- 470 Beinlich, A., Klemd, R., John, T. and Gao, J. (2010) Trace-element mobilization during
471 Ca-metasomatism along a major fluid conduit: Eclogitization of blueschist as a consequence
472 of fluid–rock interaction. *Geochimica et Cosmochimica Acta* 74, 1892-1922.
- 473 Beinlich, A., Mavromatis, V., Austrheim, H. and Oelkers, E.H. (2014) Inter-mineral Mg
474 isotope fractionation during hydrothermal ultramafic rock alteration-Implications for the
475 global Mg-cycle. *Earth and Planetary Science Letters* 392, 166-176.
- 476 Busigny, V., Cartigny, P., Philippot, P., Ader, M. and Javoy, M. (2003) Massive recycling of
477 nitrogen and other fluid-mobile elements (K, Rb, Cs, H) in a cold slab environment: evidence
478 from HP to UHP oceanic metasediments of the Schistes Lustrés nappe (western Alps,
479 Europe). *Earth and Planetary Science Letters* 215, 27-42.
- 480 Carswell, D.A. (1990) Eclogite facies rocks. Blackie and Son Ltd, pp 14-49.
- 481 Chen, Y.-X., Schertl, H.P., Zheng, Y.-F., Huang, F., Zhou, K. and Gong, Y.-Z. (2016) Mg-O
482 isotopes trace the origin of Mg-rich fluids in the deeply subducted continental crust of
483 Western Alps. *Earth and Planetary Science Letters* 456, 157-167..
- 484 Chu, Z., Chen, F., Yang, Y. and Guo, J. (2009) Precise determination of Sm, Nd
485 concentrations and Nd isotopic compositions at the nanogram level in geological samples by
486 thermal ionization mass spectrometry. *Journal of Analytical Atomic Spectrometry* 24,
487 1534-1544.
- 488 Dasgupta, R. and Hirschmann, M.M. (2010) The deep carbon cycle and melting in Earth's
489 interior. *Earth and Planetary Science Letters* 298, 1-13.
- 490 Du, J.-X., Zhang, L.-F., Shen, X.-J. and Bader, T. (2014a) A new PTt path of eclogites from
491 Chinese southwestern Tianshan: constraints from PT pseudosections and Sm-Nd isochron
492 dating. *Lithos* 200, 258-272.
- 493 Du, J., Zhang, L., Bader, T., Chen, Z. and Lü, Z. (2014b) Metamorphic evolution of relict
494 lawsonite- bearing eclogites from the (U) HP metamorphic belt in the Chinese southwestern
495 Tianshan. *Journal of Metamorphic Geology* 32, 575-598.
- 496 Du, J., Zhang, L., Lü, Z. and Chu, X. (2011) Lawsonite-bearing chloritoid–glaucophane
497 schist from SW Tianshan, China: phase equilibria and P–T path. *Journal of Asian Earth
498 Sciences* 42, 684-693.
- 499 Foster G L, Pogge von Strandmann P A E. and Rae J W B. (2010) Boron and magnesium
500 isotopic composition of seawater. *Geochemistry, Geophysics, Geosystems* 11(8),
501 DOI: 10.1029/2010GC003201.
- 502 Gao, J., John, T., Klemd, R. and Xiong, X. (2007) Mobilization of Ti–Nb–Ta during
503 subduction: evidence from rutile-bearing dehydration segregations and veins hosted in
504 eclogite, Tianshan, NW China. *Geochimica et Cosmochimica Acta* 71, 4974-4996.
- 505 Gao, J. and Klemd, R. (2001) Primary fluids entrapped at blueschist to eclogite transition:
506 evidence from the Tianshan meta-subduction complex in northwestern China. *Contributions
507 to Mineralogy and Petrology* 142, 1-14.

- 508 Gao, J. and Klemd, R. (2003) Formation of HP–LT rocks and their tectonic implications in
509 the western Tianshan Orogen, NW China: geochemical and age constraints. *Lithos* 66, 1-22.
- 510 Gao, J., Klemd, R., Zhang, L., Wang, Z. and Xiao, X. (1999) PT path of
511 high-pressure/low-temperature rocks and tectonic implications in the western Tianshan
512 Mountains, NW China. *Journal of Metamorphic Geology* 17, 621-636.
- 513 Gao, S., Zhang, B.-R., Gu, X.-M., Xie, Q.-L., Gao, C.-L. and Guo, X.-M. (1995)
514 Silurian-Devonian provenance changes of South Qinling basins: implications for accretion of
515 the Yangtze (South China) to the North China cratons. *Tectonophysics* 250, 183-197.
- 516 Gerya, T.V., Stöckhert, B. and Perchuk, A.L. (2002) Exhumation of high- pressure
517 metamorphic rocks in a subduction channel: A numerical simulation. *Tectonics* 21, 6-1-6-19.
- 518 Glodny, J., Austrheim, H., Molina, J.F., Rusin, A.I. and Seward, D. (2003) Rb/Sr record of
519 fluid-rock interaction in eclogites: The Marun-Keu complex, Polar Urals, Russia. *Geochimica
520 et Cosmochimica Acta* 67, 4353-4371.
- 521 Gorman, P.J., Kerrick, D. and Connolly, J. (2006) Modeling open system metamorphic
522 decarbonation of subducting slabs. *Geochemistry, Geophysics, Geosystems* 7.
- 523 Guo, S., Ye, K., Chen, Y., Liu, J.-B., Mao, Q. and Ma, Y.-G. (2012) Fluid-rock interaction
524 and element mobilization in UHP metabasalt: Constraints from an omphacite-epidote vein
525 and host eclogites in the Dabie orogen. *Lithos* 136-139, 145-167.
- 526 Halama, R., John, T., Herms, P., Hauff, F. and Schenk, V. (2011) A stable (Li, O) and
527 radiogenic (Sr, Nd) isotope perspective on metasomatic processes in a subducting slab.
528 *Chemical Geology* 281, 151-166.
- 529 Horodyskyj, U., Lee, C.-T.A. and Luffi, P. (2009) Geochemical evidence for exhumation of
530 eclogite via serpentinite channels in ocean-continent subduction zones. *Geosphere* 5,
531 426-438.
- 532 Hu, Y., Teng, F. -Z, Plank, T. and Huang, H.-J. (2017) Magnesium isotopic composition of
533 subducting marine sediments. *Chemical Geology*,
534 <http://dx.doi.org/10.1016/j.chemgeo.2017.06.010>
- 535 Huang, F., Chen, L., Wu, Z. and Wang, W. (2013) First-principles calculations of equilibrium
536 Mg isotope fractionations between garnet, clinopyroxene, orthopyroxene, and olivine:
537 Implications for Mg isotope thermometry. *Earth and Planetary Science Letters* 367, 61-70.
- 538 Huang, J., Ke, S., Gao, Y., Xiao, Y. and Li, S. (2015) Magnesium isotopic compositions of
539 altered oceanic basalts and gabbros from IODP site 1256 at the East Pacific Rise. *Lithos* 231,
540 53-61.
- 541 Ionov, D.A. and Seitz, H.-M. (2008) Lithium abundances and isotopic compositions in
542 mantle xenoliths from subduction and intra-plate settings: mantle sources vs. eruption
543 histories. *Earth and Planetary Science Letters* 266, 316-331.

- 544 John, T., Gussone, N., Podladchikov, Y.Y., Bebout, G.E., Dohmen, R., Halama, R., Klemd,
545 R., Magna, T. and Seitz, H.-M. (2012) Volcanic arcs fed by rapid pulsed fluid flow through
546 subducting slabs. *Nature Geoscience* 5, 489-492.
- 547 John, T., Klemd, R., Gao, J. and Garbe-Schönberg, C.-D. (2008) Trace-element mobilization
548 in slabs due to non steady-state fluid–rock interaction: constraints from an eclogite-facies
549 transport vein in blueschist (Tianshan, China). *Lithos* 103, 1-24.
- 550 John, T., Scherer, E.E., Haase, K. and Schenk, V. (2004) Trace element fractionation during
551 fluid-induced eclogitization in a subducting slab: trace element and Lu–Hf–Sm–Nd isotope
552 systematics. *Earth and Planetary Science Letters* 227, 441-456.
- 553 Kelemen, P.B. and Manning, C.E. (2015) Reevaluating carbon fluxes in subduction zones,
554 what goes down, mostly comes up. *Proceedings of the National Academy of Sciences* 112,
555 E3997-E4006.
- 556 Kelley, K.A., Plank, T., Ludden, J. and Staudigel, H. (2003) Composition of altered oceanic
557 crust at ODP Sites 801 and 1149. *Geochemistry, Geophysics, Geosystems* 4, 890, doi:
558 10.1029/2002GC000435.
- 559 Kessel, R., Schmidt, M.W., Ulmer, P. and Pettke, T. (2005) Trace element signature of
560 subduction-zone fluids, melts and supercritical liquids at 120-180 km depth. *Nature* 437,
561 724-727.
- 562 King, R.L., Bebout, G.E., Moriguti, T. and Nakamura, E. (2006) Elemental mixing
563 systematics and Sr–Nd isotope geochemistry of mélange formation: obstacles to
564 identification of fluid sources to arc volcanics. *Earth and Planetary Science Letters* 246,
565 288-304.
- 566 Klemd, R. (2013) *Metasomatism During High-Pressure Metamorphism: Eclogites and*
567 *Blueschist-Facies Rocks, Metasomatism and the Chemical Transformation of Rock*. Springer,
568 pp. 351-413.
- 569 Klemd, R., John, T., Scherer, E., Rondenay, S. and Gao, J. (2011) Changes in dip of
570 subducted slabs at depth: petrological and geochronological evidence from HP–UHP rocks
571 (Tianshan, NW-China). *Earth and Planetary Science Letters* 310, 9-20.
- 572 Lü, Z., Zhang, L., Du, J. and Bucher, K. (2009) Petrology of coesite- bearing eclogite from
573 Habutengsu Valley, western Tianshan, NW China and its tectonometamorphic implication.
574 *Journal of Metamorphic Geology* 27, 773-787.
- 575 Lü, Z., Zhang, L., Du, J., Yang, X., Tian, Z. and Xia, B. (2012) Petrology of HP metamorphic
576 veins in coesite-bearing eclogite from western Tianshan, China: fluid processes and
577 elemental mobility during exhumation in a cold subduction zone. *Lithos* 136, 168-186.
- 578 Li, J.-L., Klemd, R., Gao, J. and John, T. (2016a) Poly-cyclic Metamorphic Evolution of
579 Eclogite: Evidence for Multistage Burial–Exhumation Cycling in a Subduction Channel.
580 *Journal of Petrology* 57, 119-146.

581 Li, Q.-L., Lin, W., Su, W., Li, X.-h., Shi, Y.-H., Liu, Y. and Tang, G.-Q. (2011a) SIMS U–Pb
582 rutile age of low-temperature eclogites from southwestern Chinese Tianshan, NW China.
583 *Lithos* 122, 76-86.

584 Li, S.-G, Yang, W., Ke, S., Meng, X.-N, Tian, H.-C., Xu, L.-J., He, Y.-S., Huang, J., Wang,
585 X.-C., Xia, Q.-K., Sun, W.-D., Yang, X.-Y., Ren, Z.-Y., Wei, H.-Q., Liu, Y.-S., Meng, F.-C.
586 and Yan, J. (2017) Deep carbon cycles constrained by a large-scale mantle Mg isotope
587 anomaly in eastern China. *National Science Review* 4, 111-120.

588 Li, W.-Y., Teng, F.-Z., Ke, S., Rudnick, R.L., Gao, S., Wu, F.-Y. and Chappell, B. (2010)
589 Heterogeneous magnesium isotopic composition of the upper continental crust. *Geochimica
590 et Cosmochimica Acta* 74, 6867-6884.

591 Li, W.-Y., Teng, F.-Z., Xiao, Y. and Huang, J. (2011b) High-temperature inter-mineral
592 magnesium isotope fractionation in eclogite from the Dabie orogen, China. *Earth and
593 Planetary Science Letters* 304, 224-230.

594 Li, W.Y., Teng, F.Z., Wing, B.A. and Xiao, Y. (2014) Limited magnesium isotope
595 fractionation during metamorphic dehydration in metapelites from the Onawa contact
596 aureole, Maine. *Geochemistry, Geophysics, Geosystems* 15, 408-415.

597 Li, W. Y., Teng, F. Z., Xiao, Y., Gu, H. O., Zha, X. P. and Huang, J. (2016b) Empirical
598 calibration of the clinopyroxene–garnet magnesium isotope geothermometer and
599 implications. *Contributions to Mineralogy and Petrology* 171(7), 1-14.

600 Ling M X, Sedaghatpour F, Teng F Z., Hays, P.D., Strauss, J. and Sun, W.D. (2011)
601 Homogeneous magnesium isotopic composition of seawater: an excellent geostandard for Mg
602 isotope analysis. *Rapid Communications in Mass Spectrometry* 25(19): 2828-2836.

603 Liu, P.-P., Teng, F.-Z., Dick, HJB., Zhou M.-F. and Chung, S.-L (2017) Magnesium isotopic
604 composition of the oceanic mantle and oceanic Mg cycling. *Geochimica et Cosmochimica
605 Acta* 206, 151-165.

606 Miller, C., Stosch, H.-G. and Hoernes, S. (1988) Geochemistry and origin of eclogites from
607 the type locality Koralpe and Saualpe, Eastern Alps, Austria. *Chemical Geology* 67, 103-118.

608 Plank, T. and Langmuir, C.H. (1998) The chemical composition of subducting sediment and
609 its consequences for the crust and mantle. *Chemical geology* 145, 325-394.

610 Pogge von Strandmann, P.A.E., Elliott, T., Marschall, H.R., Coath, C., Lai, Y.-J., Jeffcoate,
611 A.B. and Ionov, D.A. (2011) Variations of Li and Mg isotope ratios in bulk chondrites and
612 mantle xenoliths. *Geochimica et Cosmochimica Acta* 75, 5247-5268.

613 Poli S. and Schmidt, M.W. (2002) Petrology of subducted slabs. *Annual Review of Earth and
614 Planetary Sciences* 30, 207-235.

615 Pogge von Strandmann, P.A.P., Dohmen, R., Marschall, H.R., Schumacher, J.C. and Elliott,
616 T. (2015) Extreme magnesium isotope fractionation at outcrop scale records the mechanism
617 and rate at which reaction fronts advance. *Journal of Petrology* 56, 33-58.

618 Simons, K.K., Harlow, G.E., Brueckner, H.K., Goldstein, S.L., Sorensen, S.S., Hemming,
619 N.G. and Langmuir, C.H. (2010) Lithium isotopes in Guatemalan and Franciscan HP–LT
620 rocks: Insights into the role of sediment-derived fluids during subduction. *Geochimica et*
621 *Cosmochimica Acta* 74, 3621-3641.

622 Su, W., Gao, J., Klemd, R., Li, J.-L., Zhang, X., Li, X.-H., Chen, N.-S. and Zhang, L. (2010)
623 U–Pb zircon geochronology of Tianshan eclogites in NW China: implication for the collision
624 between the Yili and Tarim blocks of the southwestern Altaids. *European Journal of*
625 *Mineralogy* 22, 473-478.

626 Sun, S.-S. and McDonough, W. (1989) Chemical and isotopic systematics of oceanic basalts:
627 implications for mantle composition and processes. Geological Society, London, Special
628 Publications 42, 313-345.

629 Teng, F.-Z. (2017) Magnesium isotope geochemistry. *Reviews in Mineralogy &*
630 *Geochemistry* 82, 219-287.

631 Teng, F.-Z., Hu, Y. and Chauvel, C. (2016) Magnesium isotope geochemistry in arc
632 volcanism. *Proceedings of the National Academy of Sciences*, 201518456.

633 Teng, F.-Z., Li, W.-Y., Ke, S., Marty, B., Dauphas, N., Huang, S., Wu, F.-Y. and Pourmand,
634 A. (2010) Magnesium isotopic composition of the Earth and chondrites. *Geochimica et*
635 *Cosmochimica Acta* 74, 4150-4166.

636 Teng F. -Z., Li W. Y., Ke S., Yang W., Liu S. A., Sedaghatpour F., Wang S. J., Huang K. J.,
637 Hu Y., Ling M. X., Xiao Y., Liu X. M., Li X. W., Gu H. O., Sio C., Wallace D., Su B. X.,
638 Zhao L., Harrington M. and Brewer A. (2015) Magnesium isotopic compositions of
639 international geological reference materials. *Geostandards and Geoanalytical Research* 39,
640 329-339.

641 Teng, F.-Z., Wadhwa, M. and Helz, R.T. (2007) Investigation of magnesium isotope
642 fractionation during basalt differentiation: implications for a chondritic composition of the
643 terrestrial mantle. *Earth and Planetary Science Letters* 261, 84-92.

644 Teng, F.Z. and Yang, W. (2014) Comparison of factors affecting the accuracy of
645 high- precision magnesium isotope analysis by multi- collector inductively coupled plasma
646 mass spectrometry. *Rapid Communications in Mass Spectrometry* 28, 19-24.

647 Teng, F.Z., Yang, W., Rudnick, R.L. and Hu, Y. (2013) Heterogeneous magnesium isotopic
648 composition of the lower continental crust: A xenolith perspective. *Geochemistry,*
649 *Geophysics, Geosystems* 14, 3844-3856.

650 Tipper, E., Galy, A., Gaillardet, J., Bickle, M., Elderfield, H. and Carder, E. (2006) The
651 magnesium isotope budget of the modern ocean: Constraints from riverine magnesium
652 isotope ratios. *Earth and Planetary Science Letters* 250, 241-253.

653 van der Straaten, F., Halama, R., John, T., Schenk, V., Hauff, F. and Andersen, N. (2012)
654 Tracing the effects of high-pressure metasomatic fluids and seawater alteration in
655 blueschist-facies overprinted eclogites: Implications for subduction channel processes.
656 *Chemical Geology* 292, 69-87.

657 van der Straaten, F., Schenk, V., John, T. and Gao, J. (2008) Blueschist-facies rehydration of
658 eclogites (Tian Shan, NW-China): implications for fluid–rock interaction in the subduction
659 channel. *Chemical Geology* 255, 195-219.

660 Veizer, J. (1989) Strontium isotopes in seawater through time. *Annual Review of Earth and*
661 *Planetary Sciences* 17, 141-167.

662 Wang, S.-J., Teng, F.-Z. and Li, S.-G. (2014a) Tracing carbonate–silicate interaction during
663 subduction using magnesium and oxygen isotopes. *Nature communications* 5.

664 Wang, S.-J., Teng, F.-Z., Li, S.-G. and Hong, J.-A. (2014b) Magnesium isotopic systematics
665 of mafic rocks during continental subduction. *Geochimica et Cosmochimica Acta* 143, 34-48.

666 Wang, S.-J., Teng, F.-Z., Rudnick, R.L. and Li, S.-G. (2015a) The behavior of magnesium
667 isotopes in low-grade metamorphosed mudrocks. *Geochimica et Cosmochimica Acta* 165,
668 435-448.

669 Wang, S.-J., Teng, F.-Z. and Bea, F. (2015b) Magnesium isotopic systematics of metapelite
670 in the deep crust and implications for granite petrogenesis. *Geochem. Perspect. Lett* 1, 75-83.

671 Wang, S.-J., Teng, F.-Z. and Scott, J. (2016) Tracing the origin of continental HIMU-like
672 intraplate volcanism using magnesium isotope systematics. *Geochimica et Cosmochimica*
673 *Acta* 185, 78-87.

674 Windley, B., Allen, M., Zhang, C., Zhao, Z. and Wang, G. (1990) Paleozoic accretion and
675 Cenozoic reformation of the Chinese Tien Shan range, central Asia. *Geology* 18, 128-131.

676 Xiao, Y., Lavis, S., Niu, Y., Pearce, J.A., Li, H., Wang, H. and Davidson, J. (2012)
677 Trace-element transport during subduction-zone ultrahigh-pressure metamorphism: Evidence
678 from western Tianshan, China. *Geological Society of America Bulletin* 124, 1113-1129.

679 Yang, W., Teng, F.-Z. and Zhang, H.-F. (2009) Chondritic magnesium isotopic composition
680 of the terrestrial mantle: a case study of peridotite xenoliths from the North China craton.
681 *Earth and Planetary Science Letters* 288, 475-482.

682 Yang, X., Zhang, L.F., Tian, Z.L., Bader, T., (2013) Petrology and U-Pb zircon dating of
683 coesite-bearing metapelites from the Kebuerte Valley, western Tianshan, China. *Journal of*
684 *Asian Earth Sciences* 70-71, 295-307.

685 Zack, T. and John, T. (2007) An evaluation of reactive fluid flow and trace element mobility
686 in subducting slabs. *Chemical Geology* 239, 199-216.

687 Zhang, L., Du, J., Lü, Z., Yang, X., Gou, L., Xia, B., Chen, Z., Wei, C. and Song, S. (2013) A
688 huge oceanic-type UHP metamorphic belt in southwestern Tianshan, China: Peak
689 metamorphic age and PT path. *Chinese Science Bulletin* 58, 4378-4383.

690 Zhang, L., Ellis, D.J. and Jiang, W. (2002) Ultrahigh-pressure metamorphism in western
691 Tianshan, China: Part I. Evidence from inclusions of coesite pseudomorphs in garnet and
692 from quartz exsolution lamellae in omphacite in eclogites. *American mineralogist* 87,
693 853-860.

- 694 Zhang, L-F., Ellis, D., Williams, S. and Jiang, W.-B. (2003) Ultrahigh-pressure
695 metamorphism in eclogites from the western Tianshan, China — Reply. *American*
696 *Mineralogist* 88, 1157-1160.
- 697 Zhang, L., Lü, Z., Zhang, G. and Song, S. (2008) The geological characteristics of
698 oceanic-type UHP metamorphic belts and their tectonic implications: Case studies from
699 Southwest Tianshan and North Qaidam in NW China. *Chinese Science Bulletin* 53,
700 3120-3130.
- 701 Zhang, L., Song, S., Liou, J.G., Ai, Y. and Li, X. (2005) Relict coesite exsolution in
702 omphacite from Western Tianshan eclogites, China. *American Mineralogist* 90, 181-186.
- 703 Zhang, L., Zhang, L., Lü, Z., Bader, T. and Chen, Z. (2016) Nb–Ta mobility and
704 fractionation during exhumation of UHP eclogite from southwestern Tianshan, China.
705 *Journal of Asian Earth Sciences* 122, 136-157.
- 706 Zindler, A. and Hart, S. (1986) Chemical geodynamics. *Annual review of earth and planetary*
707 *sciences* 14, 493-571.
- 708

709 **Figure Captions**

710 Fig. 1: Strontium and Nd isotopic compositions of the eclogites from southwestern Tianshan.
711 MORB and OIB fields are from Zindler and Hart (1986); $^{87}\text{Sr}/^{86}\text{Sr}$ ratio of the Ordovician to
712 Carboniferous (O-C) seawater is from Veizer (1989), and $^{87}\text{Sr}/^{86}\text{Sr}$ ratio of the global
713 subducting sediments (GLOSS) can be high as much as 0.73 (Plank and Langmuir, 1998)

714

715 Fig. 2: Histogram of $\delta^{26}\text{Mg}$ values for the eclogites from southwestern Tianshan. $\delta^{26}\text{Mg}$
716 values of the eclogites with continental origin are from Li et al. (2010) and Wang et al.
717 (2014a, b). $\delta^{26}\text{Mg}$ values of the unaltered oceanic crust are from Teng et al. (2010).

718

719 Fig. 3: Ba/Rb vs. K (a), K/Th vs. Ba/Th (b), and Ce/Pb vs. 1/Pb (c) diagrams to differentiate
720 between ancient seawater alteration and metamorphic metasomatism after Bebout (2007).
721 The Ni vs. Co diagram (d) indicates that most eclogites have lower Ni and Co concentration
722 than oceanic basalts. Data of MORB and OIB are from Sun and McDonough (1989); the Ni
723 and Co of average serpentinite are from data compiled by van der Straaten et al. (2008).

724

725 Fig. 4: Rb/Sr vs. Pb^* (a), Ba/Pb vs. Pb^* (b), $^{87}\text{Sr}/^{86}\text{Sr}_{(t)}$ vs. Pb^* (c) and $^{87}\text{Sr}/^{86}\text{Sr}_{(t)}$ vs. Rb/Sr (d)
726 diagrams to indicate the two fluid components. The Pb^* represents an indices of enrichment
727 of Pb in the eclogites: $\text{Pb}^* = 2 * \text{Pb}_N / (\text{Ce}_N + \text{Pr}_N)$. The higher the Pb^* , the more enrichment of
728 Pb for the eclogites. The carbonated eclogites are marked as dashed outline. The black

729 triangle in panels a and b represents the average altered oceanic crust (super composite of
730 Ocean Drilling Program Site 801) in Kelley et al. (2003). Black square and diamond
731 represent the composition of MORB and OIB, respectively. The component 1 is enriched in
732 LILEs, which might be derived from dehydration of mica-group minerals. The component 2
733 is enriched in Pb and $^{87}\text{Sr}/^{86}\text{Sr}$, likely released from epidote-group minerals.

734

735 Fig. 5: The variation of $\delta^{26}\text{Mg}$ values as a function of MgO content for the eclogites (yellow
736 circle) and mica schists (blue diamond) from southwestern Tianshan. The compositions of
737 altered oceanic crust (AOC) from ODP site 801 and IODP site 1256 are from Huang et al.
738 (2015) and Teng (2017). The co-variation between $\delta^{26}\text{Mg}$ and MgO for the eclogites can be
739 roughly modeled as fluid-rock interactions of the eclogites with compositionally different two
740 fluid components. We assume that the component 1, because of its origin from Mg-rich
741 mica-group minerals or to a less extent talc, have $\delta^{26}\text{Mg} = +1.00$ and $\text{MgO} = 1 \text{ wt.}\%$; the
742 component 2, released from Mg-poor epidote-group minerals, contain very little Mg
743 (assuming $\text{MgO} = 0.05 \text{ wt.}\%$). Although we assign a value of $+1.00$ for the $\delta^{26}\text{Mg}$ of the
744 low-MgO component 2, the change of this value will not affect the modelling significantly,
745 as the component 2 contains too little Mg so as not to influence the Mg isotopic composition
746 of the eclogites. Thus, the two purple curves with increment of 10% represent the fluid-rock
747 interaction of an eclogite ($\delta^{26}\text{Mg} = -0.25$; $\text{MgO} = 8 \text{ wt.}\%$) with high-MgO and low-MgO
748 fluid components, with the partition coefficient of MgO between fluid and eclogite,
749 $D_{\text{eclogite/fluid}} = 4$. The black dotted curve represents binary mixing between sediments and
750 basalts, which suggests that $>60\%$ of sedimentary component is required to produce the Mg

751 isotopic composition of the eclogites. The green bar represents the normal mantle $\delta^{26}\text{Mg}$
752 value (Teng et al., 2010).

753

754 Fig. 6: $\delta^{26}\text{Mg}$ vs. Pb^* (a), $\delta^{26}\text{Mg}$ vs. $^{87}\text{Sr}/^{86}\text{Sr}_{(t)}$ (b), $\delta^{26}\text{Mg}$ vs. Rb/Sr (c), and $\delta^{26}\text{Mg}$ vs. Ba/Pb
755 (d) diagrams showing the influence of the two fluid components on the Mg isotopic
756 systematics of eclogites (shown as solid arrows). The carbonated eclogites are marked as
757 dashed outline. The high-LILE fluid component contains a considerable amount of
758 isotopically heavy Mg to shift the $\delta^{26}\text{Mg}$ of eclogites towards a higher value, whereas the
759 high- $^{87}\text{Sr}/^{86}\text{Sr}$ and -Pb fluid component contains little heavy Mg to influence the Mg isotopic
760 systematics of eclogites. Some low-Rb/Sr and -Ba/Pb samples also have slightly heavy Mg
761 isotopic compositions, which might point towards the contributions of fluids dehydrated from
762 talc in serpentinite (shown as dashed arrows; Beinlich et al., 2014).

763

764 **Table Captions**

765 Table 1. Strontium and Nd isotopic compositions of the eclogites from southwestern
766 Tianshan.

767

768 Table 2. Magnesium isotopic compositions of the eclogites and mica schists and their mineral
769 separates from southwestern Tianshan.

1 **Tracing subduction zone fluid-rock interactions using**
2 **trace element and Mg-Sr-Nd isotopes**

3
4 Shui-Jiong Wang^{1,2*}, Fang-Zhen Teng^{2*}, Shu-Guang Li¹, Li-Fei Zhang³, Jin-Xue Du^{1,3}, Yong-Sheng
5 He¹, Yaoling Niu^{4,5}

6
7 ¹ State Key Laboratory of Geological Processes and Mineral Resources, China University of Geosciences,
8 Beijing 100083, China

9 ² Isotope Laboratory, Department of Earth and Space Sciences, University of Washington, Seattle, WA
10 98195-1310, USA

11 ³ School of Earth Space Sciences, Peking University, Beijing, China

12 ⁴ Institute of Oceanology, Chinese Academy of Sciences, Qingdao 266071, China

13 ⁵ Department of Earth Sciences, Durham University, Durham DH1 3LE, UK

14 Abstract: 492 words

15 Text: 5139 words

16 Figure: 6

17 Table: 2

18 Revised version submitted to *Lithos* (July 29, 2017)

19

20 *Present address: Department of Earth and Atmospheric Sciences, Indiana University, Bloomington, IN 47405
21 USA.

22 Corresponding authors: sxw057@gmail.com(S.-J. Wang); fteng@u.washington.edu (F.-Z. Teng)

23 **Abstract**

24 Slab-derived fluids play a key role in mass transfer and elemental/isotopic exchanges in
25 subduction zones. The exhumation of deeply subducted crust is achieved via a subduction
26 channel where fluids from various sources are abundant, and thus the chemical/isotopic
27 compositions of these rocks could have been modified by subduction-zone fluid-rock
28 interactions. Here, we investigate the Mg isotopic systematics of eclogites from southwestern
29 Tianshan, in conjunction with major/trace element and Sr-Nd isotopes, to characterize the
30 source and nature of fluids and to decipher how fluid-rock interactions in subduction channel
31 might influence the Mg isotopic systematics of exhumed eclogites. The eclogites have high
32 LILEs (especially Ba) and Pb, high initial $^{87}\text{Sr}/^{86}\text{Sr}$ (up to 0.7117; higher than that of coeval
33 seawater), and varying Ni and Co (mostly lower than those of oceanic basalts), suggesting
34 that these eclogites have interacted with metamorphic fluids mainly released from subducted
35 sediments, with minor contributions from altered oceanic crust or altered abyssal peridotites.
36 The positive correlation between $^{87}\text{Sr}/^{86}\text{Sr}$ and Pb^* (an index of Pb enrichment; $\text{Pb}^* =$
37 $2 \cdot \text{Pb}_N / [\text{Ce}_N + \text{Pr}_N]$), and the decoupling relationships and bidirectional patterns in
38 $^{87}\text{Sr}/^{86}\text{Sr}$ -Rb/Sr, Pb^* -Rb/Sr and Pb^* -Ba/Pb spaces imply the presence of two compositionally
39 different components for the fluids: one enriched in LILEs, and the other enriched in Pb and
40 $^{87}\text{Sr}/^{86}\text{Sr}$. The systematically heavier Mg isotopic compositions ($\delta^{26}\text{Mg} = -0.37$ to $+0.26$)
41 relative to oceanic basalts (-0.25 ± 0.07) and the roughly negative correlation of $\delta^{26}\text{Mg}$ with
42 MgO for the southwestern Tianshan eclogites, cannot be explained by inheritance of Mg
43 isotopic signatures from ancient seafloor alteration or prograde metamorphism. Instead, the
44 signatures are most likely produced by fluid-rock interactions during the exhumation of

45 eclogites. The high Rb/Sr and Ba/Pb but low Pb* eclogites generally have high bulk-rock
46 $\delta^{26}\text{Mg}$ values, whereas high Pb* and $^{87}\text{Sr}/^{86}\text{Sr}$ eclogites have mantle-like $\delta^{26}\text{Mg}$ values,
47 suggesting that the two fluid components have diverse influences on the Mg isotopic
48 systematics of these eclogites. The LILE-rich fluid component, possibly derived from
49 mica-group minerals, contains a considerable amount of isotopically heavy Mg that has
50 shifted the $\delta^{26}\text{Mg}$ of the eclogites towards higher values. By contrast, the $^{87}\text{Sr}/^{86}\text{Sr}$ - and
51 Pb-rich fluid component, most likely released from epidote-group minerals in metasediments,
52 has little Mg so as not to modify the Mg isotopic composition of the eclogites. In addition,
53 the influence of talc-derived fluid might be evident in a very few eclogites that have low
54 Rb/Sr and Ba/Pb but slightly heavier Mg isotopic compositions. These findings represent an
55 important step toward a broad understanding of the Mg isotope geochemistry in subduction
56 zones, and contributing to understanding why island arc basalts have averagely heavier Mg
57 isotopic compositions than the normal mantle.

58 **Keywords:** Mg isotopes, subduction channel, fluid-rock interaction, eclogite, Tianshan

59 **1. Introduction**

60 Subduction channel is a highly reactive interface between subducting oceanic
61 lithosphere and mantle wedge, in which mass transfer as well as elemental and isotopic
62 exchanges actively occur (*e.g.*, Bebout and Penniston-Dorland, 2016). In this region, fluids
63 released from various subducting slab lithologies (*e.g.*, sediments, altered oceanic crust, and
64 altered abyssal peridotites) can be mixed and penetrate into exhuming rocks, inducing
65 extensive fluid-rock interactions (Zack and John, 2007; John et al., 2008; van der Straaten et
66 al., 2008, 2012). The fluids, when emanating from the interface into the mantle wedge, can
67 further impart their chemical/isotopic signatures to the juxtaposed mantle rocks and
68 associated arc volcanism.

69 Trace elements in conjunction with Sr-Nd-O isotopic systematics have been widely used
70 to identify and understand fluid-rock interactions in subduction channels (Glodny et al., 2003;
71 John et al., 2004, 2012; King et al., 2006; Halama et al., 2011). The magnesium (Mg)
72 isotopic systematics might be a useful tracer of subduction-zone fluid-rock interactions,
73 potentially providing insights into the source and nature of fluids. Magnesium is fluid-mobile
74 at low temperatures, which leads to large Mg isotope fractionations as much as 7 ‰ during
75 Earth's surface processes (Teng, 2017 and references therein). Recent studies also
76 documented high mobility of Mg during subduction-zone metamorphism (van der Straaten et
77 al., 2008; Horodyskyj et al., 2009; Pogge von Strandmann et al., 2015; Chen et al., 2016).
78 Chen et al. (2016) found high $\delta^{26}\text{Mg}$ values (up to +0.72) for white schists from Western
79 Alps, and linked them to infiltration of Mg-rich fluids derived from dehydration of

80 serpentinites. Recent studies also documented generally heavier Mg isotopic compositions in
81 arc volcanic rocks relative to normal peridotitic sources ($\delta^{26}\text{Mg} = -0.25 \pm 0.07$), which were
82 explained as the addition of heavy Mg isotopes from subducting slabs to the mantle wedge
83 (Teng et al., 2016; Li et al., 2017). A general conclusion derived from these studies is that the
84 subduction-zone fluids might be isotopically heavy in terms of Mg isotopes. Nevertheless,
85 the interpretation of any Mg isotopic variations in subduction-related rocks requires the
86 knowledge of how Mg isotopes behave in subduction channels, and how fluid-rock
87 interactions could affect the Mg isotopic systematics of a rock.

88 Orogenic eclogites of seafloor protolith may be the best choice to study subduction
89 channel processes. Oceanic crust undergoes seawater alteration prior to subduction and is,
90 therefore, more hydrated relative to the continental crust (Miller et al., 1988). It experiences
91 extensive dehydration together with the sediment veneer during subduction (Gerya et al.,
92 2002). In addition, the exhumation of oceanic crust via the subduction channel proceeds at
93 relatively slower rate (mm/yr; Agard et al., 2009). All of these allow eclogites of seafloor
94 protolith to preserve a record of extensive fluid-rock interactions during exhumation. An
95 increasing number of studies have shown that fluid-rock interactions can readily modify the
96 chemical and isotopic compositions of exhumed eclogites (*e.g.*, Bebout, 2007; Xiao et al.,
97 2012; Klemd, 2013), although how the chemical/isotopic composition shift depends on the
98 nature and abundance of fluids with which the eclogites have interacted.

99 In this study, we investigate a suite of well-characterized eclogites/blueschists and mica
100 schists from southwestern Tianshan, China. We present the first Mg isotopic data for the

101 orogenic eclogites of seafloor protolith, and in combination with Sr-Nd isotopic and trace
102 elemental data, we explore the influence of subduction-zone fluid-rock interactions on the
103 Mg isotopic systematics of eclogites. Our results show that these eclogites are variably
104 enriched in heavy Mg isotopes, which may result from interactions of the eclogites with both
105 high-MgO and low-MgO fluids released from different hydrous minerals in the subduction
106 channel.

107 **2. Geological settings and samples**

108 The high-pressure to ultrahigh-pressure (HP-UHP) metamorphic belt of Chinese
109 southwestern Tianshan, located along the suture between the Yili and the Tarim blocks, was
110 formed during the northward subduction of the Palaeo-South Tianshan oceanic crust beneath
111 the Yili block (Windley et al., 1990; Gao et al., 1999; Zhang et al., 2002, 2008). The eclogites
112 and retrograded blueschists in southwestern Tianshan occur as interlayers or lenticular bodies
113 in mica schists, representing the relic oceanic crust that experienced subduction and
114 exhumation in response to later continental collision. The protoliths of eclogites and
115 associated blueschists range from MORBs to OIBs as indicated by the geochemical data and
116 their preserved pillow structures in the field (Zhang et al., 2002, 2008; Gao and Klemd, 2003;
117 Ai et al., 2006). The eclogites and their host rocks have experienced peak coesite-bearing
118 eclogite-facies metamorphism at 324 ~ 312 Ma (Zhang et al., 2005; Su et al., 2010; Klemd et
119 al., 2011; Li et al., 2011a; Yang et al., 2013), followed by a slow exhumation rate to
120 amphibolite-facies between 320 Ma and 240 Ma (*e.g.*, Zhang et al., 2013). The peak and
121 retrograde metamorphic temperatures estimated for the southwestern Tianshan eclogites vary

122 from 450 to 630 °C (*e.g.*, Du et al., 2014a, b). The retrograde metamorphic temperatures are
123 slightly higher than the peak-eclogite facies temperatures as a result of thermal relaxation
124 during the exhumation (*e.g.*, Zhang et al., 2013). The presence of abundant millimeter to
125 decimeter-wide and centimeter to meter-long veins in southwestern Tianshan blueschists and
126 eclogites indicates extensive fluid-rock interactions and fluid-mediated mass transport during
127 crustal subduction and exhumation (Gao and Klemd, 2001; Gao et al., 2007; John et al., 2008;
128 2012; Beinlich et al., 2010; Lü et al., 2012).

129 The petrology and metamorphic evolution of the studied eclogites and mica schists have
130 been well characterized (Zhang et al., 2003; Ai et al., 2006; Lü et al., 2009; Du et al., 2011,
131 2014b; Xiao et al., 2012). The eclogites consist mainly of garnet, omphacite, glaucophane,
132 paragonite, epidote, calcite, dolomite and quartz/coesite; the mica schists are mainly
133 composed of garnet, glaucophane, phengite, epidote, paragonite, plagioclase and
134 quartz/coesite. A detail description of the studied eclogites and mica schists including the
135 sample localities has been given in Supplementary Table S1.

136 **3. Analytical methods**

137 **3.1 Major and trace elements**

138 Major elements were analyzed at the Hebei Institute of Regional Geology and Mineral
139 Resources, China, by wavelength dispersive X-Ray fluorescence spectrometry (Gao et al.,
140 1995). Analytical uncertainties are generally better than 1%. The H₂O⁺ and CO₂ were
141 determined by gravimetric methods and potentiometry, respectively. Trace elements were
142 analyzed using an Elan 6100 DRC ICP-MS at the CAS key laboratory of crust-material and

143 environments, University of Science and Technology of China, Hefei. Samples were
144 analyzed with aliquots of USGS whole-rock standards BHVO-2, BIR-1, AGV-2 and GSP-2,
145 which were treated as unknown. Results for the USGS standards together with the reference
146 values are reported in Supplementary Table S2. Analytical uncertainties are better than 5%
147 for most of the elements.

148 **3.2 Strontium and Nd isotopic analysis**

149 The Sr and Nd were separated from the matrix with cation exchange chromatography
150 with Bio-Rad AG50W-X12 resin using the method described by Chu et al. (2009). The Sr
151 and Nd isotopes were performed using an Isoprobe-T thermal ionization mass spectrometer
152 (TIMS) at the State Key Laboratory of Lithospheric Evolution, Institute of Geology and
153 Geophysics, Chinese Academy of Sciences. Measured $^{87}\text{Sr}/^{86}\text{Sr}$ and $^{143}\text{Nd}/^{144}\text{Nd}$ ratios were
154 corrected for mass-fractionation using $^{86}\text{Sr}/^{88}\text{Sr} = 0.1194$ and $^{146}\text{Nd}/^{144}\text{Nd} = 0.7219$,
155 respectively. During the course of this study, standards of NBS987-Sr and jNdi-Nd give a
156 value of $^{87}\text{Sr}/^{86}\text{Sr} = 0.710245 \pm 20$ and $^{143}\text{Nd}/^{144}\text{Nd} = 0.512117 \pm 10$, respectively.

157 **3.3 Magnesium isotopic analysis**

158 Magnesium isotopic ratios were analyzed for bulk rock powders and mineral separates
159 at the University of Washington, Seattle. The separation of Mg was achieved by cation
160 exchange chromatography using Bio-Rad AG50W-X8 resin in 1N HNO₃ media (Teng et al.,
161 2007, 2010a; 2015; Yang et al., 2009; Li et al., 2010). Two standards, Kilbourne Hole (KH)
162 olivine and seawater, were processed together with samples for each batch of column
163 chemistry. The Mg isotopic ratios were determined using the standard-sample bracketing

164 protocol on a *Nu* plasma MC-ICPMS (Teng and Yang, 2014). The blank Mg signal for ^{24}Mg
165 was $< 10^{-4}$ V, which is negligible relative to the sample signals of 3-5 V. The KH olivine and
166 seawater yielded average $\delta^{26}\text{Mg}$ of -0.25 ± 0.05 and -0.82 ± 0.06 , respectively, consistent
167 with previous reported values (Foster et al., 2010; Li et al., 2010; Teng et al., 2010; Ling et
168 al., 2011; Wang et al., 2016)

169 **4. Results**

170 Major and trace elemental compositions of the eclogites and mica schists are
171 summarized in Supplementary Table S3. The eclogites have SiO_2 ranging from 39.82 to
172 52.47 wt.% and MgO ranging from 3.19 to 9.68 wt.% (Supplementary Table S3), and plot in
173 subalkalic basalt field in Zr/Ti versus Nb/Y diagram (Supplementary Fig. S1; Pearce, 1996).
174 The high contents of H_2O^+ (0.58 to 3.38 wt.%) and CO_2 (0.08 to 8.96 wt.%) are consistent
175 with the presence of water- and/or carbon oxide-bearing minerals such as zoisite/clinozoisite
176 and calcite/dolomite. The eclogites have variably high LILEs (*e.g.*, Ba, Rb, Cs, and K) and
177 Pb, but low Ni and Co concentrations (Supplementary Table S3). The mica schists are felsic
178 with SiO_2 ranging from 59.53 to 76.66 wt.% and MgO ranging from 1.81 to 3.60 wt.%
179 (Supplementary Table S3). They are characterized by variable contents of LILEs, Sr and Pb,
180 which may be controlled by different proportions of mica-group minerals (host of LILEs) and
181 epidote-group minerals (major host of Sr and Pb) in southwestern Tianshan metasediments
182 (*e.g.*, Xiao et al., 2012).

183 The Sr and Nd isotopic compositions of the eclogites are reported in Table 1. The
184 eclogites have positive age-corrected $\epsilon\text{Nd}_{320\text{Ma}}$ value ranging from +2.8 to +10.1 (with one

185 exception of -2.4; Fig. 1). They have extremely high and variable initial Sr isotopic
186 compositions ($^{87}\text{Sr}/^{86}\text{Sr}_{320\text{Ma}}$) varying from 0.7058 to 0.7117 (Fig. 1), a range that is even
187 higher than that of Ordovician to Carboniferous seawater ($^{87}\text{Sr}/^{86}\text{Sr} = 0.7075 - 0.7090$; Veizer,
188 1989). As a result, the eclogites plot rightward far from the field defined by depleted MORB
189 and OIB in $\epsilon\text{Nd}(t) - ^{87}\text{Sr}/^{86}\text{Sr}(t)$ diagram (Fig. 1).

190 The $\delta^{26}\text{Mg}$ values of southwestern Tianshan eclogites vary widely from -0.37 ± 0.05 to
191 $+0.26 \pm 0.04$ (Table 2), equal to or higher than unaltered oceanic basalts and eclogites of
192 continental basalt protolith, both of which have homogeneous Mg isotopic compositions
193 around the normal mantle value (-0.25 ± 0.07 ; Fig. 2). Garnets in southwestern Tianshan
194 eclogites yield $\delta^{26}\text{Mg}$ values varying from -1.75 ± 0.07 to -1.10 ± 0.07 , and omphacites have
195 $\delta^{26}\text{Mg}$ values ranging from -0.04 ± 0.05 to $+0.46 \pm 0.07$ (Table 2), with corresponding
196 inter-mineral Mg isotope fractionation ($\Delta^{26}\text{Mg}_{\text{Cpx-Grt}} = \delta^{26}\text{Mg}_{\text{Cpx}} - \delta^{26}\text{Mg}_{\text{Grt}}$) in the range of
197 1.23 - 1.98. Temperatures estimated using garnet-clinopyroxene Mg isotope geothermometer
198 range from 485°C to 675°C (Huang et al., 2013; Li et al., 2016b) , which are in rough
199 agreement with the peak and retrograde metamorphic temperatures for the Tianshan eclogites
200 (*e.g.*, Du et al., 2014a, b). Six mica schists from southwestern Tianshan have bulk $\delta^{26}\text{Mg}$
201 values ranging from -0.11 ± 0.05 to $+0.23 \pm 0.02$ (Table 2).

202 **5. Discussion**

203 The overprint of fluid-rock interactions on the southwestern Tianshan
204 eclogites/blueschists has been confirmed by many petrological and geochemical studies (John
205 et al., 2008; van der Straaten et al., 2008, 2012; Beinlich et al., 2010; Lü et al., 2012; Li et al.,

206 2016a; Zhang et al., 2016). Depending on the nature and abundance of fluids in a subduction
207 channel, the initial composition of an eclogite can be altered to various degrees after
208 fluid-rock interactions. In this section, we first focus on the trace element and Sr-Nd isotopes
209 to characterize the source and nature of the fluids, and then decipher how fluid-rock
210 interactions may have influenced the Mg isotopic systematics of the eclogites. Finally, we
211 discuss the Mg isotope geochemistry of slab-derived fluids in the subduction channel and
212 their influences on the sub-arc peridotites.

213 **5.1 Geochemical evidence for fluid-rock interactions**

214 Trace element and Sr-Nd isotope geochemistry suggest interactions of eclogites with
215 metamorphic fluids. The fluids are mainly derived from subducted sediments, with limited
216 contributions from serpentinites or altered oceanic crusts. Most eclogites are variably
217 enriched in LILEs (*e.g.*, Ba, Cs, Rb, and K) and Pb (Fig. 3), which can be produced during
218 either ancient seafloor alteration or subduction-zone fluid-rock interactions. Bebout (2007)
219 documented that significant enrichments of Ba and Pb in metabasaltic rocks can be most
220 directly associated with metasomatism because these two elements are only slightly enriched
221 in altered oceanic basalts during seafloor alteration relative to other LILEs. The consistently
222 high Ba/Rb, high Ba/K and low Ce/Pb of our eclogites are thus indicative of HP/UHP
223 fluid-rock interactions rather than ancient seawater alteration (Fig. 3a, b, c). Furthermore,
224 these eclogites have extremely high initial $^{87}\text{Sr}/^{86}\text{Sr}$ ratio up to 0.7117 (Fig. 1), a signature
225 that cannot be attributed to pre-subduction seawater alteration because the
226 Ordovician-Carboniferous seawater has much lower $^{87}\text{Sr}/^{86}\text{Sr}$ ratios of 0.7075 - 0.7090

227 (Veizer, 1989). The high $^{87}\text{Sr}/^{86}\text{Sr}_{320\text{Ma}}$ ratios thus must have resulted from interactions of the
228 eclogites with fluids during metasomatism, and the fluids might be derived from subducted
229 sediments whose $^{87}\text{Sr}/^{86}\text{Sr}$ ratios can be as high as 0.73 (Plank and Langmuir, 1998). In
230 contrast to Sr isotopes, Nd isotopes appear to behave conservatively during the metasomatism
231 (King et al., 2006). Due to the low mobility of REE during metamorphic dehydration under
232 relatively low P-T conditions (Kessel et al., 2005), slab-derived fluids would contain too little
233 Nd to affect the Nd isotopic systematics of eclogites (van der Straaten et al., 2012), such that
234 the eclogites retain their depleted Nd isotopic signatures (Fig. 1). In accordance with the high
235 $^{87}\text{Sr}/^{86}\text{Sr}$ ratios, most eclogites contain very low concentrations of Co and Ni evolving from
236 oceanic basalts towards the GLOSS (global subducting sediments; Fig. 3d), pointing towards
237 again interactions of the eclogites with sediment-derived fluids. Some eclogites however
238 have Ni and Co contents overlapping or slightly higher than oceanic basalts (Fig. 3d). This
239 indicates the possible contributions of altered oceanic crust-derived or serpentinite-derived
240 fluids (*e.g.*, van der Straaten et al., 2012), although subducted sediments must be the
241 dominant source for fluids that have interacted with the eclogites.

242 The geochemical signatures of sediment-derived fluids might vary significantly in
243 response to the mineralogical heterogeneity of subducting sediments. The eclogites display a
244 series of geochemical features indicative of two compositionally different fluid components
245 (Fig. 4). As shown in Rb/Sr vs. Pb^* (an index of enrichment of Pb; $\text{Pb}^* = 2 \cdot \text{Pb}_N / [\text{Ce}_N + \text{Pr}_N]$)
246 and Ba/Pb vs. Pb^* diagrams, the enrichment of Pb in eclogites is not always associated with
247 the enrichment of LILEs (Fig. 4a and b). The observed decoupling patterns may indicate two
248 major fluid components: one enriched in LILEs relative to Pb (*e.g.*, high Rb/Sr and Ba/Pb but

249 low Pb*), and the other enriched in Pb relative to LILEs (*e.g.*, high Pb* but low Rb/Sr or
250 Ba/Pb). The roughly positive correlation between Pb* and $^{87}\text{Sr}/^{86}\text{Sr}_{320\text{Ma}}$ (Fig. 4c), suggests
251 that the high-Pb component also contains a significant amount of radiogenic Sr that has
252 elevated the $^{87}\text{Sr}/^{86}\text{Sr}$ value of eclogites. Some carbonated eclogites are extremely enriched in
253 elemental Sr but have relatively low $^{87}\text{Sr}/^{86}\text{Sr}$ values of 0.7066 – 0.7078 (Supplementary Fig.
254 S2), suggesting that the surrounding marbles are not the source of high- $^{87}\text{Sr}/^{86}\text{Sr}$ fluid. Instead,
255 the high- $^{87}\text{Sr}/^{86}\text{Sr}$ fluid component must be sourced from other metasediments, such as mica
256 schists. The high-LILEs component, on the other hand, might contain too little Sr to modify
257 the Sr isotopic composition of eclogites, as reflected by the decoupling relationship between
258 $^{87}\text{Sr}/^{86}\text{Sr}_{320\text{Ma}}$ and Rb/Sr (Fig. 4d): the high-Rb/Sr eclogites display low $^{87}\text{Sr}/^{86}\text{Sr}_{320\text{Ma}}$ values,
259 whereas the low-Rb/Sr samples are characterized by highly radiogenic Sr isotopic
260 compositions (Fig. 4d). All these observations support that the eclogites were infiltrated by
261 two fluid components. The distinct geochemical signatures of the two fluid components are
262 consistent with the fact that LILEs and Sr-Pb are hosted in different hydrous minerals in
263 subducted sediments: mica-group minerals are the dominant host for LILEs, whereas
264 epidote-group minerals (and to a less extent carbonate minerals and paragonite) are the major
265 host of Pb and Sr (*e.g.*, Busigny et al., 2003; Bebout et al., 2007, 2013; Xiao et al., 2012). As
266 a result, fluid dehydrated from mica-group minerals would have high Rb/Sr and Ba/Pb ratios,
267 whereas fluid released from epidote-group minerals in metasediments could be enriched in
268 Pb and Sr (as well as $^{87}\text{Sr}/^{86}\text{Sr}$). It is possible that varying modal mineralogy in the subducted
269 sediments (*e.g.*, mica-group minerals are abundant in metapelites and epidote-group minerals
270 are abundant in greywackes) can result in decomposition of mica- and epidote-group

271 minerals in different proportions along the subduction P-T path and generate the two fluid
272 components in the subduction channel. During crustal subduction, biotite is thought to be
273 completely decomposed at $P = 1.3-1.5$ GPa, at which the epidote-group minerals such as
274 epidote and zoisite are still stable (Poli and Schmidt, 2002). Therefore, decomposition of
275 biotite at the early stage during crustal subduction could release a significant amount of fluid
276 that is enriched in LILEs. At a higher pressure above 2.5 GPa, epidote and zoisite might
277 become unstable (Carswell, 1990; Poli and Schmidt, 2002). Metamorphic dehydration at this
278 stage could thus release abundant Sr and Pb to the fluids. Such fluids, when released from
279 subducting oceanic crust, would migrate upward along the subduction channel, infiltrate the
280 exhuming eclogites and impart their distinct geochemical signatures to the eclogites via
281 fluid-rock interactions.

282 **5.2 Constraining the mechanisms of Mg isotopic variations in the eclogites**

283 The eclogites have varying Mg contents ($MgO = 3.2$ to 9.7 wt.%) at a given SiO_2
284 content, and more variable and systemically heavier Mg isotopic composition than fresh
285 oceanic basalts (Fig. 5). The simplest explanation for the low MgO and high $\delta^{26}Mg$ of
286 eclogites is physical/mechanical mixing with a high- $\delta^{26}Mg$ sedimentary component at some
287 point before or during the exhumation of the eclogites. However, this is very unlikely
288 because binary mixing calculation, using the highest $\delta^{26}Mg$ value of the six mica schists as an
289 endmember (Q-314), suggests that at least $>60\%$ of sedimentary component is required to
290 produce the Mg isotopic compositions of most eclogites (Fig. 5), such that the eclogites
291 would have anomalously high SiO_2 contents (>55 wt.%). In addition, the SiO_2 of eclogites

292 does not correlate with neither $^{87}\text{Sr}/^{86}\text{Sr}_{320\text{Ma}}$ nor $\epsilon\text{Nd}(t)$ (Supplementary Fig. S3), further
293 supporting that binary mixing between basalt (or eclogite) and sediment (or metasediment)
294 might not be the case. Magnesium is fluid-mobile, thus, processes like ancient seawater
295 alteration, prograde metamorphism (*e.g.*, release of Mg into metamorphic fluids and
296 eclogite-host isotopic exchanges), and retrograde fluid-rock interactions (*e.g.*, interaction
297 with metamorphic fluid during exhumation), could potentially account for the observed Mg
298 isotopic variations. Next, we endeavor to explore how Mg isotopes behave during these
299 processes, based on which, we highlight the importance of subduction channel fluids in
300 generating Mg isotopic variations in exhumed eclogites.

301 *5.2.1 Seafloor alteration cannot explain the Mg isotopic signatures*

302 Seafloor alteration produces even larger Mg isotopic variations, with Mg isotopes likely
303 fractionated in a different manner from that observed in the eclogites, as shown in Fig. 5.
304 Altered oceanic crusts (AOC) from two different sites have been reported for Mg isotopic
305 compositions (Huang et al., 2015; Teng, 2017). Carbonate-barren AOC samples recovered
306 from IODP site 1256 in the eastern equatorial Pacific retain a mantle-like $\delta^{26}\text{Mg}$ value as for
307 fresh oceanic basalts (Fig. 5; Huang et al., 2015), based on which Huang et al. (2015)
308 concluded that seafloor alteration causes limited Mg isotope fractionation, regardless of
309 alteration temperature and water/rock ratio. At the other site (ODP site 801) in western
310 Pacific, extensively altered AOC samples have highly variable $\delta^{26}\text{Mg}$ values ranging from
311 -2.76 to +0.21 (Fig. 5), with low $\delta^{26}\text{Mg}$ values being associated with carbonate enriched
312 samples and high $\delta^{26}\text{Mg}$ values associated with clay-rich samples (Teng, 2017). Due to

313 carbonate dilution effect (Tipper et al., 2006), the AOC samples from ODP site 801 are
314 distributed in a trend in which $\delta^{26}\text{Mg}$ values decrease as MgO decreases (Fig. 5). Different
315 from AOC, none of the studied eclogites (32 in total) show enrichment of light Mg isotopes,
316 although they contain variable abundances of carbonate minerals. Furthermore, neither
317 heavily nor less altered AOC could account for the roughly negative correlation between
318 $\delta^{26}\text{Mg}$ and MgO for the eclogites (Fig. 5). Thus, ancient seawater alteration is unlikely to be
319 the cause of the variable and systemically heavier Mg isotopic compositions of the eclogites.

320 *5.2.2 The role of prograde metamorphic dehydration and eclogite-host isotopic exchange*

321 Magnesium isotope fractionation during prograde metamorphic dehydration or
322 eclogite-host isotopic exchange cannot account for the Mg isotopic variations in our eclogites.
323 It is possible that dehydrated fluids have distinct Mg isotopic compositions from the rock
324 where the fluids are from. However, since the fraction of Mg partitioning into the fluid
325 phases is so small compared to that inherited by metamorphic minerals during prograde
326 metamorphism, metamorphic dehydration causes insignificant Mg isotope fractionation ($<$
327 ± 0.07) on a bulk-rock scale (Li et al., 2011b, 2014; Teng et al., 2013; Wang et al., 2014b,
328 2015a, b). Local isotopic exchange between eclogite and its host rock can potentially change
329 the original mantle-like Mg isotopic compositions of the eclogites (Wang et al., 2014a). To
330 which direction the Mg isotopes of the eclogites fractionate depends on the types of host rock.
331 For example, eclogite-host isotopic exchange would make eclogite boudins in
332 carbonates/marbles isotopically lighter, whereas those enclosed in mica schists heavier
333 (Wang et al., 2014a). However, no systemic relationship between $\delta^{26}\text{Mg}$ and host rock type

334 was observed for the southwestern Tianshan eclogites. On the opposite, the carbonated
335 eclogites (those enclosed in marbles) in our study are enriched in heavy Mg isotopes ($\delta^{26}\text{Mg}$
336 = -0.28 to +0.02; Table 2), which we interpret below as a result of infiltration of external
337 fluids derived from metasediments.

338 *5.2.3 Response of Mg isotopic systematics in the eclogites to fluid-rock interactions.*

339 Thus, our favored interpretation of the Mg isotopic variation is fluid-rock interaction in
340 a subduction channel. The fluids must be enriched in heavy Mg isotopes, and pervasively
341 reactive in interacting with the eclogites because the eclogites have systemically heavier Mg
342 isotopic compositions (Fig. 2), regardless of their diverse host rock types. Below, we discuss
343 how the two fluid components may have affected the Mg isotopic compositions of the
344 eclogites.

345 The two fluid components, due to their derivation from different hydrous minerals,
346 have different impacts on the Mg isotopic systematics of eclogites. In the plots of $\delta^{26}\text{Mg}$ vs.
347 Pb^* and $\delta^{26}\text{Mg}$ vs. $^{87}\text{Sr}/^{86}\text{Sr}_{320\text{Ma}}$ (Fig. 6a and b), the high- Pb^* and $^{87}\text{Sr}/^{86}\text{Sr}_{320\text{Ma}}$ samples
348 retain a mantle-like $\delta^{26}\text{Mg}$ value, suggesting that the infiltration of high-Pb and $^{87}\text{Sr}/^{86}\text{Sr}$ fluid
349 component had limited influences on the Mg isotopic composition of eclogites. Being the
350 dominant source of high-Pb and $^{87}\text{Sr}/^{86}\text{Sr}$ component, the epidote-group minerals contain
351 little Mg (*e.g.*, Guo et al., 2012), and thus the fluid dehydrated from them is unable to modify
352 the Mg isotopic composition of the eclogites (although the exact $\delta^{26}\text{Mg}$ value of any
353 epidote-group mineral has not been reported so far). The low- Pb^* and $^{87}\text{Sr}/^{86}\text{Sr}_{320\text{Ma}}$ samples,
354 on the other hand, have variably high $\delta^{26}\text{Mg}$ values (Fig. 6a and b). As expected, eclogites

355 with high-Rb/Sr and Ba/Pb ratios have high $\delta^{26}\text{Mg}$ values (Fig. 6c and d). Because of the
356 complexity of the fluid system and the uncertainty of its Mg concentration and Mg isotopic
357 composition, we are not expecting to see good correlations between $\delta^{26}\text{Mg}$ and indices of
358 enrichment of LILEs (such as Rb/Sr and Ba/Pb). However, the general patterns shown in Fig.
359 6c and d suggest that the high-LILEs component carries a significant amount of isotopically
360 heavy Mg that has elevated the $\delta^{26}\text{Mg}$ values of the eclogites. Mica-group minerals, as the
361 major source of high-LILE component, are enriched in MgO, and in addition their $\delta^{26}\text{Mg}$
362 values are characteristically high. For instance, biotites in metapelites from the Ivrea Zone in
363 NW Italy have $\delta^{26}\text{Mg}$ values ranging from -0.08 to +1.10 (Wang et al., 2015b), and phengites
364 in eclogites from the Dabie orogen have $\delta^{26}\text{Mg}$ values of +0.30 to +0.59 (Li et al., 2011b).
365 Therefore, eclogites metasomatized by the mica-derived fluid could gain high- $\delta^{26}\text{Mg}$
366 signatures. It is also important to note that in Fig. 6c and d, a part of low-Rb/Sr and Ba/Pb
367 samples has slightly high $\delta^{26}\text{Mg}$ value, which we interpret as the possible influence of the
368 talc-derived fluid, as the talc in serpentinite is depleted in LILEs but enriched in heavy Mg
369 ($\delta^{26}\text{Mg} = +0.06$ to +0.30; Beinlich et al., 2014). Without good constraints on the Mg isotopic
370 composition of fluid and the partition coefficient of MgO between fluid and eclogite, it is not
371 yet possible to give a perfect fluid-rock interaction model for the whole dataset of the
372 eclogites. However, the rough negative correlation between $\delta^{26}\text{Mg}$ and MgO for the eclogites
373 can be generally modeled as interactions of eclogites with high-MgO (*e.g.*, dehydrated from
374 mica-group minerals or talc) and low-MgO fluid components (*e.g.*, dehydrated from
375 epidote-group minerals) under a variety of water/rock (fluid/eclogite) ratios (Fig. 5).

376 **5.3 The origins of isotopically heavy fluids in subduction channel**

377 Fluids in subduction channels are likely to have heavy Mg isotopic compositions,
378 although different subducted lithologies themselves show highly variable $\delta^{26}\text{Mg}$ values. The
379 subducted abyssal peridotites have slightly high $\delta^{26}\text{Mg}$ values of -0.25 - +0.10 (Liu et al.,
380 2017). The subducted sediments and altered oceanic crusts have large variations in $\delta^{26}\text{Mg}$
381 values (-2.76 ‰ to +0.92 ‰), with low $\delta^{26}\text{Mg}$ associated with carbonated rocks and with
382 high $\delta^{26}\text{Mg}$ associated with carbonate-free rocks (Li et al., 2010; Wang et al., 2015a; Huang
383 et al., 2015; Teng et al., 2016; Hu et al., 2017; Teng, 2017). One might expect that subsolidus
384 decarbonation or carbonate dissolution during metamorphism could release light Mg isotopes,
385 making the sediment-derived fluids isotopically light. However, decarbonation is an
386 inefficient process for carbonated sediments/basalts along the P-T paths of oceanic
387 subduction (Gorman et al., 2006; Dasgupta and Hirschmann, 2010). Carbonate species
388 dissolved in metamorphic fluid is thought to be mainly CaCO_3 (Ague and Nicolescu, 2014;
389 Kelemen and Manning, 2015; Li et al., 2017). Therefore, the presence of carbonate minerals
390 in subducted rocks has negligible influence on the Mg isotopic composition of dehydrated
391 fluids (Li et al., 2017). By contrast, breakdown of hydrous minerals might control the Mg
392 concentration and Mg isotopic composition of dehydrated fluids. Reported $\delta^{26}\text{Mg}$ values for
393 Mg-rich hydrous minerals, such like mica-group minerals and talc, are higher than the normal
394 mantle value (Li et al., 2011b; Beinlich et al., 2014; Wang et al., 2015b), and thus it is very
395 likely that the dehydrated fluids are enriched in heavy Mg isotopes. For example, a recent
396 study suggested that the fluid derived from talc and antigorite in serpentinite is likely
397 characterized by high-Mg and high- $\delta^{26}\text{Mg}$, and could be responsible for the high $\delta^{26}\text{Mg}$
398 values of white schists in Western Alps (Chen et al., 2016).

399 **5.4 Implications on Mg isotopic systematics in sub-arc peridotites**

400 Fluids in subduction channels can infiltrate the mantle wedge, inducing fluid-peridotite
401 interactions and potentially modifying the Mg isotopic composition of associated peridotites.
402 Only a few Mg isotopic data have been reported so far for mantle wedge peridotites, and they
403 are indeed enriched in heavy Mg isotopes: six arc peridotites from Avacha Volcano in
404 Kamchatka analyzed by Pogge von Strandmann et al. (2011) have $\delta^{26}\text{Mg}$ values ranging from
405 -0.25 to -0.06, higher than the normal mantle value (-0.25 ± 0.07 ; Teng et al., 2010).
406 Although the actual mechanism responsible for the Mg isotopic variations in these peridotites
407 is still uncertain, their high $\delta^{26}\text{Mg}$ values are consistent with petrological and geochemical
408 evidence suggesting that these peridotites have been affected by upward fluid migration from
409 the subducting slab (Ionov and Seitz, 2008). Most recently, Li et al. (2017) found that island
410 arc or back arc basin basalts from circum-Pacific arcs, including Kamchatka, Philippines,
411 Costa Rica and Lau Basin have generally high $\delta^{26}\text{Mg}$ values ranging from -0.35 to +0.06.
412 Teng et al. (2016) reported the Martinique arc lava $\delta^{26}\text{Mg}$ values of -0.25 to -0.10. Those
413 values overlap the Avacha peridotites and are systemically higher than normal oceanic
414 basalts and peridotites, consistent with the interpretation that isotopically heavy fluids
415 released from the subducted slab incorporate into the mantle wedge (Teng et al., 2016; Li et
416 al., 2017). All the three cases suggest that massive flux of dehydrated fluid into the sub-arc
417 mantle could facilitate extensive fluid-peridotite interaction and shift the $\delta^{26}\text{Mg}$ of sub-arc
418 peridotite towards higher values.

419 **6. Conclusions**

420 To reveal the nature of fluid-rock interactions in subduction channels and the influence
421 of subduction-zone fluids on the Mg isotopic systematics in exhumed rocks, we present
422 major and trace elements, and Sr-Nd-Mg isotopic data for the eclogites and mica schists from
423 southwestern Tianshan, China. The following conclusions can be drawn:

424 (1) The eclogites have high Ba/Rb and Ba/K but low Ce/Pb ratios, suggesting the
425 overprint of subduction-zone metamorphic metasomatism. The highly radiogenic Sr
426 isotopic composition ($^{87}\text{Sr}/^{86}\text{Sr}_{320\text{Ma}} = 0.7058\text{-}0.7117$; higher than that of coeval
427 seawater), together with the varying and mostly low Ni and Co concentrations,
428 further indicate that the eclogites have interacted with fluids mainly released from
429 subducted sediments, with limited contributions from altered oceanic crust- or
430 serpentinite-derived fluids.

431 (2) The positive correlation between $^{87}\text{Sr}/^{86}\text{Sr}$ and Pb^* , and the bidirectional patterns in
432 $^{87}\text{Sr}/^{86}\text{Sr} - \text{Rb}/\text{Sr}$, $\text{Pb}^* - \text{Rb}/\text{Sr}$, and $\text{Pb}^* - \text{Ba}/\text{Pb}$ spaces, suggest interaction of the
433 eclogites with compositionally different two fluid components: the high-LILEs
434 component which could be derived from dehydration of mica-group minerals, and
435 the high-Pb and $^{87}\text{Sr}/^{86}\text{Sr}$ component likely released from epidote-group minerals in
436 subducted sediments.

437 (3) The highly variable and systemically heavy Mg isotopic compositions of eclogites
438 ($\delta^{26}\text{Mg} = -0.37$ to $+0.26$ ‰) resulted from fluid-rock interactions in the subduction
439 channel. The high-LILE component, dehydrated from Mg-rich mica-group minerals
440 or to a less extent from talc, contains a considerable amount of Mg that has shifted
441 the $\delta^{26}\text{Mg}$ of the eclogites towards higher values. The high-Pb and $^{87}\text{Sr}/^{86}\text{Sr}$

442 component, dehydrated from Mg-poor epidote-group minerals, has little Mg so as
443 not to influence the Mg isotopic composition of the eclogites.

444 **Acknowledgement**

445 The authors would like to thank two anonymous reviewers for insightful comments and
446 Editor Sun-Lin Chung for careful and efficient handling. This study was financially
447 supported by National Natural Science Foundation of China (41230209) to SGL, National
448 Science Foundation (EAR-1340160) to FZT, and National Science Foundation of China
449 (Grants 41330210, 41520104004) and Major State Basic Research Development Program
450 (Grant 2015CB856105) to LFZ.

451 **Reference**

- 452 Agard, P., Yamato, P., Jolivet, L. and Burov, E. (2009) Exhumation of oceanic blueschists
453 and eclogites in subduction zones: timing and mechanisms. *Earth-Science Reviews* 92,
454 53-79.
- 455 Ague, J.J. and Nicolescu, S. (2014) Carbon dioxide released from subduction zones by
456 fluid-mediated reactions. *Nature Geoscience* 7, 355-360.
- 457 Ai, Y.L., Zhang, L.F., Li, X.P., Qu, J.F., (2006) Geochemical characteristics and tectonic
458 implications of HP-UHP eclogites and blueschists in southwestern Tianshan, China. *Progress*
459 *in Natural Science* 16, 624-632.
- 460 Bebout, G.E. (2007) Metamorphic chemical geodynamics of subduction zones. *Earth and*
461 *Planetary Science Letters* 260, 373-393.
- 462 Bebout, G.E., Agard, P., Kobayashi, K., Moriguti, T. and Nakamura, E. (2013)
463 Devolatilization history and trace element mobility in deeply subducted sedimentary rocks:
464 Evidence from Western Alps HP/UHP suites. *Chemical Geology* 342, 1-20.
- 465 Bebout, G.E., Bebout, A.E. and Graham, C.M. (2007) Cycling of B, Li, and LILE (K, Cs, Rb,
466 Ba, Sr) into subduction zones: SIMS evidence from micas in high-P/T metasedimentary
467 rocks. *Chemical Geology* 239, 284-304.
- 468 Bebout, G.E. and Penniston-Dorland, S.C. (2016) Fluid and mass transfer at subduction
469 interfaces—The field metamorphic record. *Lithos* 240–243, 228-258.

- 470 Beinlich, A., Klemd, R., John, T. and Gao, J. (2010) Trace-element mobilization during
471 Ca-metasomatism along a major fluid conduit: Eclogitization of blueschist as a consequence
472 of fluid–rock interaction. *Geochimica et Cosmochimica Acta* 74, 1892-1922.
- 473 Beinlich, A., Mavromatis, V., Austrheim, H. and Oelkers, E.H. (2014) Inter-mineral Mg
474 isotope fractionation during hydrothermal ultramafic rock alteration-Implications for the
475 global Mg-cycle. *Earth and Planetary Science Letters* 392, 166-176.
- 476 Busigny, V., Cartigny, P., Philippot, P., Ader, M. and Javoy, M. (2003) Massive recycling of
477 nitrogen and other fluid-mobile elements (K, Rb, Cs, H) in a cold slab environment: evidence
478 from HP to UHP oceanic metasediments of the Schistes Lustrés nappe (western Alps,
479 Europe). *Earth and Planetary Science Letters* 215, 27-42.
- 480 Carswell, D.A. (1990) Eclogite facies rocks. Blackie and Son Ltd, pp 14-49.
- 481 Chen, Y.-X., Schertl, H.P., Zheng, Y.-F., Huang, F., Zhou, K. and Gong, Y.-Z. (2016) Mg-O
482 isotopes trace the origin of Mg-rich fluids in the deeply subducted continental crust of
483 Western Alps. *Earth and Planetary Science Letters* 456, 157-167..
- 484 Chu, Z., Chen, F., Yang, Y. and Guo, J. (2009) Precise determination of Sm, Nd
485 concentrations and Nd isotopic compositions at the nanogram level in geological samples by
486 thermal ionization mass spectrometry. *Journal of Analytical Atomic Spectrometry* 24,
487 1534-1544.
- 488 Dasgupta, R. and Hirschmann, M.M. (2010) The deep carbon cycle and melting in Earth's
489 interior. *Earth and Planetary Science Letters* 298, 1-13.
- 490 Du, J.-X., Zhang, L.-F., Shen, X.-J. and Bader, T. (2014a) A new PTt path of eclogites from
491 Chinese southwestern Tianshan: constraints from PT pseudosections and Sm-Nd isochron
492 dating. *Lithos* 200, 258-272.
- 493 Du, J., Zhang, L., Bader, T., Chen, Z. and Lü, Z. (2014b) Metamorphic evolution of relict
494 lawsonite- bearing eclogites from the (U) HP metamorphic belt in the Chinese southwestern
495 Tianshan. *Journal of Metamorphic Geology* 32, 575-598.
- 496 Du, J., Zhang, L., Lü, Z. and Chu, X. (2011) Lawsonite-bearing chloritoid–glaucophane
497 schist from SW Tianshan, China: phase equilibria and P–T path. *Journal of Asian Earth*
498 *Sciences* 42, 684-693.
- 499 Foster G L, Pogge von Strandmann P A E. and Rae J W B. (2010) Boron and magnesium
500 isotopic composition of seawater. *Geochemistry, Geophysics, Geosystems* 11(8),
501 DOI: 10.1029/2010GC003201.
- 502 Gao, J., John, T., Klemd, R. and Xiong, X. (2007) Mobilization of Ti–Nb–Ta during
503 subduction: evidence from rutile-bearing dehydration segregations and veins hosted in
504 eclogite, Tianshan, NW China. *Geochimica et Cosmochimica Acta* 71, 4974-4996.
- 505 Gao, J. and Klemd, R. (2001) Primary fluids entrapped at blueschist to eclogite transition:
506 evidence from the Tianshan meta-subduction complex in northwestern China. *Contributions*
507 *to Mineralogy and Petrology* 142, 1-14.

- 508 Gao, J. and Klemd, R. (2003) Formation of HP–LT rocks and their tectonic implications in
509 the western Tianshan Orogen, NW China: geochemical and age constraints. *Lithos* 66, 1-22.
- 510 Gao, J., Klemd, R., Zhang, L., Wang, Z. and Xiao, X. (1999) PT path of
511 high-pressure/low-temperature rocks and tectonic implications in the western Tianshan
512 Mountains, NW China. *Journal of Metamorphic Geology* 17, 621-636.
- 513 Gao, S., Zhang, B.-R., Gu, X.-M., Xie, Q.-L., Gao, C.-L. and Guo, X.-M. (1995)
514 Silurian-Devonian provenance changes of South Qinling basins: implications for accretion of
515 the Yangtze (South China) to the North China cratons. *Tectonophysics* 250, 183-197.
- 516 Gerya, T.V., Stöckhert, B. and Perchuk, A.L. (2002) Exhumation of high- pressure
517 metamorphic rocks in a subduction channel: A numerical simulation. *Tectonics* 21, 6-1-6-19.
- 518 Glodny, J., Austrheim, H., Molina, J.F., Rusin, A.I. and Seward, D. (2003) Rb/Sr record of
519 fluid-rock interaction in eclogites: The Marun-Keu complex, Polar Urals, Russia. *Geochimica
520 et Cosmochimica Acta* 67, 4353-4371.
- 521 Gorman, P.J., Kerrick, D. and Connolly, J. (2006) Modeling open system metamorphic
522 decarbonation of subducting slabs. *Geochemistry, Geophysics, Geosystems* 7.
- 523 Guo, S., Ye, K., Chen, Y., Liu, J.-B., Mao, Q. and Ma, Y.-G. (2012) Fluid-rock interaction
524 and element mobilization in UHP metabasalt: Constraints from an omphacite-epidote vein
525 and host eclogites in the Dabie orogen. *Lithos* 136-139, 145-167.
- 526 Halama, R., John, T., Herms, P., Hauff, F. and Schenk, V. (2011) A stable (Li, O) and
527 radiogenic (Sr, Nd) isotope perspective on metasomatic processes in a subducting slab.
528 *Chemical Geology* 281, 151-166.
- 529 Horodyskyj, U., Lee, C.-T.A. and Luffi, P. (2009) Geochemical evidence for exhumation of
530 eclogite via serpentinite channels in ocean-continent subduction zones. *Geosphere* 5,
531 426-438.
- 532 Hu, Y., Teng, F. -Z, Plank, T. and Huang, H.-J. (2017) Magnesium isotopic composition of
533 subducting marine sediments. *Chemical Geology*,
534 <http://dx.doi.org/10.1016/j.chemgeo.2017.06.010>
- 535 Huang, F., Chen, L., Wu, Z. and Wang, W. (2013) First-principles calculations of equilibrium
536 Mg isotope fractionations between garnet, clinopyroxene, orthopyroxene, and olivine:
537 Implications for Mg isotope thermometry. *Earth and Planetary Science Letters* 367, 61-70.
- 538 Huang, J., Ke, S., Gao, Y., Xiao, Y. and Li, S. (2015) Magnesium isotopic compositions of
539 altered oceanic basalts and gabbros from IODP site 1256 at the East Pacific Rise. *Lithos* 231,
540 53-61.
- 541 Ionov, D.A. and Seitz, H.-M. (2008) Lithium abundances and isotopic compositions in
542 mantle xenoliths from subduction and intra-plate settings: mantle sources vs. eruption
543 histories. *Earth and Planetary Science Letters* 266, 316-331.

- 544 John, T., Gussone, N., Podladchikov, Y.Y., Bebout, G.E., Dohmen, R., Halama, R., Klemd,
545 R., Magna, T. and Seitz, H.-M. (2012) Volcanic arcs fed by rapid pulsed fluid flow through
546 subducting slabs. *Nature Geoscience* 5, 489-492.
- 547 John, T., Klemd, R., Gao, J. and Garbe-Schönberg, C.-D. (2008) Trace-element mobilization
548 in slabs due to non steady-state fluid–rock interaction: constraints from an eclogite-facies
549 transport vein in blueschist (Tianshan, China). *Lithos* 103, 1-24.
- 550 John, T., Scherer, E.E., Haase, K. and Schenk, V. (2004) Trace element fractionation during
551 fluid-induced eclogitization in a subducting slab: trace element and Lu–Hf–Sm–Nd isotope
552 systematics. *Earth and Planetary Science Letters* 227, 441-456.
- 553 Kelemen, P.B. and Manning, C.E. (2015) Reevaluating carbon fluxes in subduction zones,
554 what goes down, mostly comes up. *Proceedings of the National Academy of Sciences* 112,
555 E3997-E4006.
- 556 Kelley, K.A., Plank, T., Ludden, J. and Staudigel, H. (2003) Composition of altered oceanic
557 crust at ODP Sites 801 and 1149. *Geochemistry, Geophysics, Geosystems* 4, 890, doi:
558 10.1029/2002GC000435.
- 559 Kessel, R., Schmidt, M.W., Ulmer, P. and Pettke, T. (2005) Trace element signature of
560 subduction-zone fluids, melts and supercritical liquids at 120-180 km depth. *Nature* 437,
561 724-727.
- 562 King, R.L., Bebout, G.E., Moriguti, T. and Nakamura, E. (2006) Elemental mixing
563 systematics and Sr–Nd isotope geochemistry of mélange formation: obstacles to
564 identification of fluid sources to arc volcanics. *Earth and Planetary Science Letters* 246,
565 288-304.
- 566 Klemd, R. (2013) *Metasomatism During High-Pressure Metamorphism: Eclogites and*
567 *Blueschist-Facies Rocks, Metasomatism and the Chemical Transformation of Rock*. Springer,
568 pp. 351-413.
- 569 Klemd, R., John, T., Scherer, E., Rondenay, S. and Gao, J. (2011) Changes in dip of
570 subducted slabs at depth: petrological and geochronological evidence from HP–UHP rocks
571 (Tianshan, NW-China). *Earth and Planetary Science Letters* 310, 9-20.
- 572 Lü, Z., Zhang, L., Du, J. and Bucher, K. (2009) Petrology of coesite- bearing eclogite from
573 Habutengsu Valley, western Tianshan, NW China and its tectonometamorphic implication.
574 *Journal of Metamorphic Geology* 27, 773-787.
- 575 Lü, Z., Zhang, L., Du, J., Yang, X., Tian, Z. and Xia, B. (2012) Petrology of HP metamorphic
576 veins in coesite-bearing eclogite from western Tianshan, China: fluid processes and
577 elemental mobility during exhumation in a cold subduction zone. *Lithos* 136, 168-186.
- 578 Li, J.-L., Klemd, R., Gao, J. and John, T. (2016a) Poly-cyclic Metamorphic Evolution of
579 Eclogite: Evidence for Multistage Burial–Exhumation Cycling in a Subduction Channel.
580 *Journal of Petrology* 57, 119-146.

581 Li, Q.-L., Lin, W., Su, W., Li, X.-h., Shi, Y.-H., Liu, Y. and Tang, G.-Q. (2011a) SIMS U–Pb
582 rutile age of low-temperature eclogites from southwestern Chinese Tianshan, NW China.
583 *Lithos* 122, 76-86.

584 Li, S.-G, Yang, W., Ke, S., Meng, X.-N, Tian, H.-C., Xu, L.-J., He, Y.-S., Huang, J., Wang,
585 X.-C., Xia, Q.-K., Sun, W.-D., Yang, X.-Y., Ren, Z.-Y., Wei, H.-Q., Liu, Y.-S., Meng, F.-C.
586 and Yan, J. (2017) Deep carbon cycles constrained by a large-scale mantle Mg isotope
587 anomaly in eastern China. *National Science Review* 4, 111-120.

588 Li, W.-Y., Teng, F.-Z., Ke, S., Rudnick, R.L., Gao, S., Wu, F.-Y. and Chappell, B. (2010)
589 Heterogeneous magnesium isotopic composition of the upper continental crust. *Geochimica
590 et Cosmochimica Acta* 74, 6867-6884.

591 Li, W.-Y., Teng, F.-Z., Xiao, Y. and Huang, J. (2011b) High-temperature inter-mineral
592 magnesium isotope fractionation in eclogite from the Dabie orogen, China. *Earth and
593 Planetary Science Letters* 304, 224-230.

594 Li, W.Y., Teng, F.Z., Wing, B.A. and Xiao, Y. (2014) Limited magnesium isotope
595 fractionation during metamorphic dehydration in metapelites from the Onawa contact
596 aureole, Maine. *Geochemistry, Geophysics, Geosystems* 15, 408-415.

597 Li, W. Y., Teng, F. Z., Xiao, Y., Gu, H. O., Zha, X. P. and Huang, J. (2016b) Empirical
598 calibration of the clinopyroxene–garnet magnesium isotope geothermometer and
599 implications. *Contributions to Mineralogy and Petrology* 171(7), 1-14.

600 Ling M X, Sedaghatpour F, Teng F Z., Hays, P.D., Strauss, J. and Sun, W.D. (2011)
601 Homogeneous magnesium isotopic composition of seawater: an excellent geostandard for Mg
602 isotope analysis. *Rapid Communications in Mass Spectrometry* 25(19): 2828-2836.

603 Liu, P.-P., Teng, F.-Z., Dick, HJB., Zhou M.-F. and Chung, S.-L (2017) Magnesium isotopic
604 composition of the oceanic mantle and oceanic Mg cycling. *Geochimica et Cosmochimica
605 Acta* 206, 151-165.

606 Miller, C., Stosch, H.-G. and Hoernes, S. (1988) Geochemistry and origin of eclogites from
607 the type locality Koralpe and Saualpe, Eastern Alps, Austria. *Chemical Geology* 67, 103-118.

608 Plank, T. and Langmuir, C.H. (1998) The chemical composition of subducting sediment and
609 its consequences for the crust and mantle. *Chemical geology* 145, 325-394.

610 Pogge von Strandmann, P.A.E., Elliott, T., Marschall, H.R., Coath, C., Lai, Y.-J., Jeffcoate,
611 A.B. and Ionov, D.A. (2011) Variations of Li and Mg isotope ratios in bulk chondrites and
612 mantle xenoliths. *Geochimica et Cosmochimica Acta* 75, 5247-5268.

613 Poli S. and Schmidt, M.W. (2002) Petrology of subducted slabs. *Annual Review of Earth and
614 Planetary Sciences* 30, 207-235.

615 Pogge von Strandmann, P.A.P., Dohmen, R., Marschall, H.R., Schumacher, J.C. and Elliott,
616 T. (2015) Extreme magnesium isotope fractionation at outcrop scale records the mechanism
617 and rate at which reaction fronts advance. *Journal of Petrology* 56, 33-58.

618 Simons, K.K., Harlow, G.E., Brueckner, H.K., Goldstein, S.L., Sorensen, S.S., Hemming,
619 N.G. and Langmuir, C.H. (2010) Lithium isotopes in Guatemalan and Franciscan HP–LT
620 rocks: Insights into the role of sediment-derived fluids during subduction. *Geochimica et*
621 *Cosmochimica Acta* 74, 3621-3641.

622 Su, W., Gao, J., Klemd, R., Li, J.-L., Zhang, X., Li, X.-H., Chen, N.-S. and Zhang, L. (2010)
623 U–Pb zircon geochronology of Tianshan eclogites in NW China: implication for the collision
624 between the Yili and Tarim blocks of the southwestern Altaids. *European Journal of*
625 *Mineralogy* 22, 473-478.

626 Sun, S.-S. and McDonough, W. (1989) Chemical and isotopic systematics of oceanic basalts:
627 implications for mantle composition and processes. Geological Society, London, Special
628 Publications 42, 313-345.

629 Teng, F.-Z. (2017) Magnesium isotope geochemistry. *Reviews in Mineralogy &*
630 *Geochemistry* 82, 219-287.

631 Teng, F.-Z., Hu, Y. and Chauvel, C. (2016) Magnesium isotope geochemistry in arc
632 volcanism. *Proceedings of the National Academy of Sciences*, 201518456.

633 Teng, F.-Z., Li, W.-Y., Ke, S., Marty, B., Dauphas, N., Huang, S., Wu, F.-Y. and Pourmand,
634 A. (2010) Magnesium isotopic composition of the Earth and chondrites. *Geochimica et*
635 *Cosmochimica Acta* 74, 4150-4166.

636 Teng F. -Z., Li W. Y., Ke S., Yang W., Liu S. A., Sedaghatpour F., Wang S. J., Huang K. J.,
637 Hu Y., Ling M. X., Xiao Y., Liu X. M., Li X. W., Gu H. O., Sio C., Wallace D., Su B. X.,
638 Zhao L., Harrington M. and Brewer A. (2015) Magnesium isotopic compositions of
639 international geological reference materials. *Geostandards and Geoanalytical Research* 39,
640 329-339.

641 Teng, F.-Z., Wadhwa, M. and Helz, R.T. (2007) Investigation of magnesium isotope
642 fractionation during basalt differentiation: implications for a chondritic composition of the
643 terrestrial mantle. *Earth and Planetary Science Letters* 261, 84-92.

644 Teng, F.Z. and Yang, W. (2014) Comparison of factors affecting the accuracy of
645 high- precision magnesium isotope analysis by multi- collector inductively coupled plasma
646 mass spectrometry. *Rapid Communications in Mass Spectrometry* 28, 19-24.

647 Teng, F.Z., Yang, W., Rudnick, R.L. and Hu, Y. (2013) Heterogeneous magnesium isotopic
648 composition of the lower continental crust: A xenolith perspective. *Geochemistry,*
649 *Geophysics, Geosystems* 14, 3844-3856.

650 Tipper, E., Galy, A., Gaillardet, J., Bickle, M., Elderfield, H. and Carder, E. (2006) The
651 magnesium isotope budget of the modern ocean: Constraints from riverine magnesium
652 isotope ratios. *Earth and Planetary Science Letters* 250, 241-253.

653 van der Straaten, F., Halama, R., John, T., Schenk, V., Hauff, F. and Andersen, N. (2012)
654 Tracing the effects of high-pressure metasomatic fluids and seawater alteration in
655 blueschist-facies overprinted eclogites: Implications for subduction channel processes.
656 *Chemical Geology* 292, 69-87.

- 657 van der Straaten, F., Schenk, V., John, T. and Gao, J. (2008) Blueschist-facies rehydration of
658 eclogites (Tian Shan, NW-China): implications for fluid–rock interaction in the subduction
659 channel. *Chemical Geology* 255, 195-219.
- 660 Veizer, J. (1989) Strontium isotopes in seawater through time. *Annual Review of Earth and*
661 *Planetary Sciences* 17, 141-167.
- 662 Wang, S.-J., Teng, F.-Z. and Li, S.-G. (2014a) Tracing carbonate–silicate interaction during
663 subduction using magnesium and oxygen isotopes. *Nature communications* 5.
- 664 Wang, S.-J., Teng, F.-Z., Li, S.-G. and Hong, J.-A. (2014b) Magnesium isotopic systematics
665 of mafic rocks during continental subduction. *Geochimica et Cosmochimica Acta* 143, 34-48.
- 666 Wang, S.-J., Teng, F.-Z., Rudnick, R.L. and Li, S.-G. (2015a) The behavior of magnesium
667 isotopes in low-grade metamorphosed mudrocks. *Geochimica et Cosmochimica Acta* 165,
668 435-448.
- 669 Wang, S.-J., Teng, F.-Z. and Bea, F. (2015b) Magnesium isotopic systematics of metapelite
670 in the deep crust and implications for granite petrogenesis. *Geochem. Perspect. Lett* 1, 75-83.
- 671 Wang, S.-J., Teng, F.-Z. and Scott, J. (2016) Tracing the origin of continental HIMU-like
672 intraplate volcanism using magnesium isotope systematics. *Geochimica et Cosmochimica*
673 *Acta* 185, 78-87.
- 674 Windley, B., Allen, M., Zhang, C., Zhao, Z. and Wang, G. (1990) Paleozoic accretion and
675 Cenozoic reformation of the Chinese Tien Shan range, central Asia. *Geology* 18, 128-131.
- 676 Xiao, Y., Lavis, S., Niu, Y., Pearce, J.A., Li, H., Wang, H. and Davidson, J. (2012)
677 Trace-element transport during subduction-zone ultrahigh-pressure metamorphism: Evidence
678 from western Tianshan, China. *Geological Society of America Bulletin* 124, 1113-1129.
- 679 Yang, W., Teng, F.-Z. and Zhang, H.-F. (2009) Chondritic magnesium isotopic composition
680 of the terrestrial mantle: a case study of peridotite xenoliths from the North China craton.
681 *Earth and Planetary Science Letters* 288, 475-482.
- 682 Yang, X., Zhang, L.F., Tian, Z.L., Bader, T., (2013) Petrology and U-Pb zircon dating of
683 coesite-bearing metapelites from the Kebuerte Valley, western Tianshan, China. *Journal of*
684 *Asian Earth Sciences* 70-71, 295-307.
- 685 Zack, T. and John, T. (2007) An evaluation of reactive fluid flow and trace element mobility
686 in subducting slabs. *Chemical Geology* 239, 199-216.
- 687 Zhang, L., Du, J., Lü, Z., Yang, X., Gou, L., Xia, B., Chen, Z., Wei, C. and Song, S. (2013) A
688 huge oceanic-type UHP metamorphic belt in southwestern Tianshan, China: Peak
689 metamorphic age and PT path. *Chinese Science Bulletin* 58, 4378-4383.
- 690 Zhang, L., Ellis, D.J. and Jiang, W. (2002) Ultrahigh-pressure metamorphism in western
691 Tianshan, China: Part I. Evidence from inclusions of coesite pseudomorphs in garnet and
692 from quartz exsolution lamellae in omphacite in eclogites. *American mineralogist* 87,
693 853-860.

- 694 Zhang, L-F., Ellis, D., Williams, S. and Jiang, W.-B. (2003) Ultrahigh-pressure
695 metamorphism in eclogites from the western Tianshan, China — Reply. *American*
696 *Mineralogist* 88, 1157-1160.
- 697 Zhang, L., Lü, Z., Zhang, G. and Song, S. (2008) The geological characteristics of
698 oceanic-type UHP metamorphic belts and their tectonic implications: Case studies from
699 Southwest Tianshan and North Qaidam in NW China. *Chinese Science Bulletin* 53,
700 3120-3130.
- 701 Zhang, L., Song, S., Liou, J.G., Ai, Y. and Li, X. (2005) Relict coesite exsolution in
702 omphacite from Western Tianshan eclogites, China. *American Mineralogist* 90, 181-186.
- 703 Zhang, L., Zhang, L., Lü, Z., Bader, T. and Chen, Z. (2016) Nb–Ta mobility and
704 fractionation during exhumation of UHP eclogite from southwestern Tianshan, China.
705 *Journal of Asian Earth Sciences* 122, 136-157.
- 706 Zindler, A. and Hart, S. (1986) Chemical geodynamics. *Annual review of earth and planetary*
707 *sciences* 14, 493-571.
- 708

709 **Figure Captions**

710 Fig. 1: Strontium and Nd isotopic compositions of the eclogites from southwestern Tianshan.
711 MORB and OIB fields are from Zindler and Hart (1986); $^{87}\text{Sr}/^{86}\text{Sr}$ ratio of the Ordovician to
712 Carboniferous (O-C) seawater is from Veizer (1989), and $^{87}\text{Sr}/^{86}\text{Sr}$ ratio of the global
713 subducting sediments (GLOSS) can be high as much as 0.73 (Plank and Langmuir, 1998)

714

715 Fig. 2: Histogram of $\delta^{26}\text{Mg}$ values for the eclogites from southwestern Tianshan. $\delta^{26}\text{Mg}$
716 values of the eclogites with continental origin are from Li et al. (2010) and Wang et al.
717 (2014a, b). $\delta^{26}\text{Mg}$ values of the unaltered oceanic crust are from Teng et al. (2010).

718

719 Fig. 3: Ba/Rb vs. K (a), K/Th vs. Ba/Th (b), and Ce/Pb vs. 1/Pb (c) diagrams to differentiate
720 between ancient seawater alteration and metamorphic metasomatism after Bebout (2007).
721 The Ni vs. Co diagram (d) indicates that most eclogites have lower Ni and Co concentration
722 than oceanic basalts. Data of MORB and OIB are from Sun and McDonough (1989); the Ni
723 and Co of average serpentinite are from data compiled by van der Straaten et al. (2008).

724

725 Fig. 4: Rb/Sr vs. Pb^* (a), Ba/Pb vs. Pb^* (b), $^{87}\text{Sr}/^{86}\text{Sr}_{(t)}$ vs. Pb^* (c) and $^{87}\text{Sr}/^{86}\text{Sr}_{(t)}$ vs. Rb/Sr (d)
726 diagrams to indicate the two fluid components. The Pb^* represents an indices of enrichment
727 of Pb in the eclogites: $\text{Pb}^* = 2 * \text{Pb}_N / (\text{Ce}_N + \text{Pr}_N)$. The higher the Pb^* , the more enrichment of
728 Pb for the eclogites. The carbonated eclogites are marked as dashed outline. The black

729 triangle in panels a and b represents the average altered oceanic crust (super composite of
730 Ocean Drilling Program Site 801) in Kelley et al. (2003). Black square and diamond
731 represent the composition of MORB and OIB, respectively. The component 1 is enriched in
732 LILEs, which might be derived from dehydration of mica-group minerals. The component 2
733 is enriched in Pb and $^{87}\text{Sr}/^{86}\text{Sr}$, likely released from epidote-group minerals.

734

735 Fig. 5: The variation of $\delta^{26}\text{Mg}$ values as a function of MgO content for the eclogites (yellow
736 circle) and mica schists (blue diamond) from southwestern Tianshan. The compositions of
737 altered oceanic crust (AOC) from ODP site 801 and IODP site 1256 are from Huang et al.
738 (2015) and Teng (2017). The co-variation between $\delta^{26}\text{Mg}$ and MgO for the eclogites can be
739 roughly modeled as fluid-rock interactions of the eclogites with compositionally different two
740 fluid components. We assume that the component 1, because of its origin from Mg-rich
741 mica-group minerals or to a less extent talc, have $\delta^{26}\text{Mg} = +1.00$ and $\text{MgO} = 1 \text{ wt.}\%$; the
742 component 2, released from Mg-poor epidote-group minerals, contain very little Mg
743 (assuming $\text{MgO} = 0.05 \text{ wt.}\%$). Although we assign a value of $+1.00$ for the $\delta^{26}\text{Mg}$ of the
744 low-MgO component 2, the change of this value will not affect the modelling significantly,
745 as the component 2 contains too little Mg so as not to influence the Mg isotopic composition
746 of the eclogites. Thus, the two purple curves with increment of 10% represent the fluid-rock
747 interaction of an eclogite ($\delta^{26}\text{Mg} = -0.25$; $\text{MgO} = 8 \text{ wt.}\%$) with high-MgO and low-MgO
748 fluid components, with the partition coefficient of MgO between fluid and eclogite,
749 $D_{\text{eclogite/fluid}} = 4$. The black dotted curve represents binary mixing between sediments and
750 basalts, which suggests that $>60\%$ of sedimentary component is required to produce the Mg

751 isotopic composition of the eclogites. The green bar represents the normal mantle $\delta^{26}\text{Mg}$
752 value (Teng et al., 2010).

753

754 Fig. 6: $\delta^{26}\text{Mg}$ vs. Pb^* (a), $\delta^{26}\text{Mg}$ vs. $^{87}\text{Sr}/^{86}\text{Sr}_{(t)}$ (b), $\delta^{26}\text{Mg}$ vs. Rb/Sr (c), and $\delta^{26}\text{Mg}$ vs. Ba/Pb
755 (d) diagrams showing the influence of the two fluid components on the Mg isotopic
756 systematics of eclogites (shown as solid arrows). The carbonated eclogites are marked as
757 dashed outline. The high-LILE fluid component contains a considerable amount of
758 isotopically heavy Mg to shift the $\delta^{26}\text{Mg}$ of eclogites towards a higher value, whereas the
759 high- $^{87}\text{Sr}/^{86}\text{Sr}$ and -Pb fluid component contains little heavy Mg to influence the Mg isotopic
760 systematics of eclogites. Some low-Rb/Sr and -Ba/Pb samples also have slightly heavy Mg
761 isotopic compositions, which might point towards the contributions of fluids dehydrated from
762 talc in serpentinite (shown as dashed arrows; Beinlich et al., 2014).

763

764 **Table Captions**

765 Table 1. Strontium and Nd isotopic compositions of the eclogites from southwestern
766 Tianshan.

767

768 Table 2. Magnesium isotopic compositions of the eclogites and mica schists and their mineral
769 separates from southwestern Tianshan.

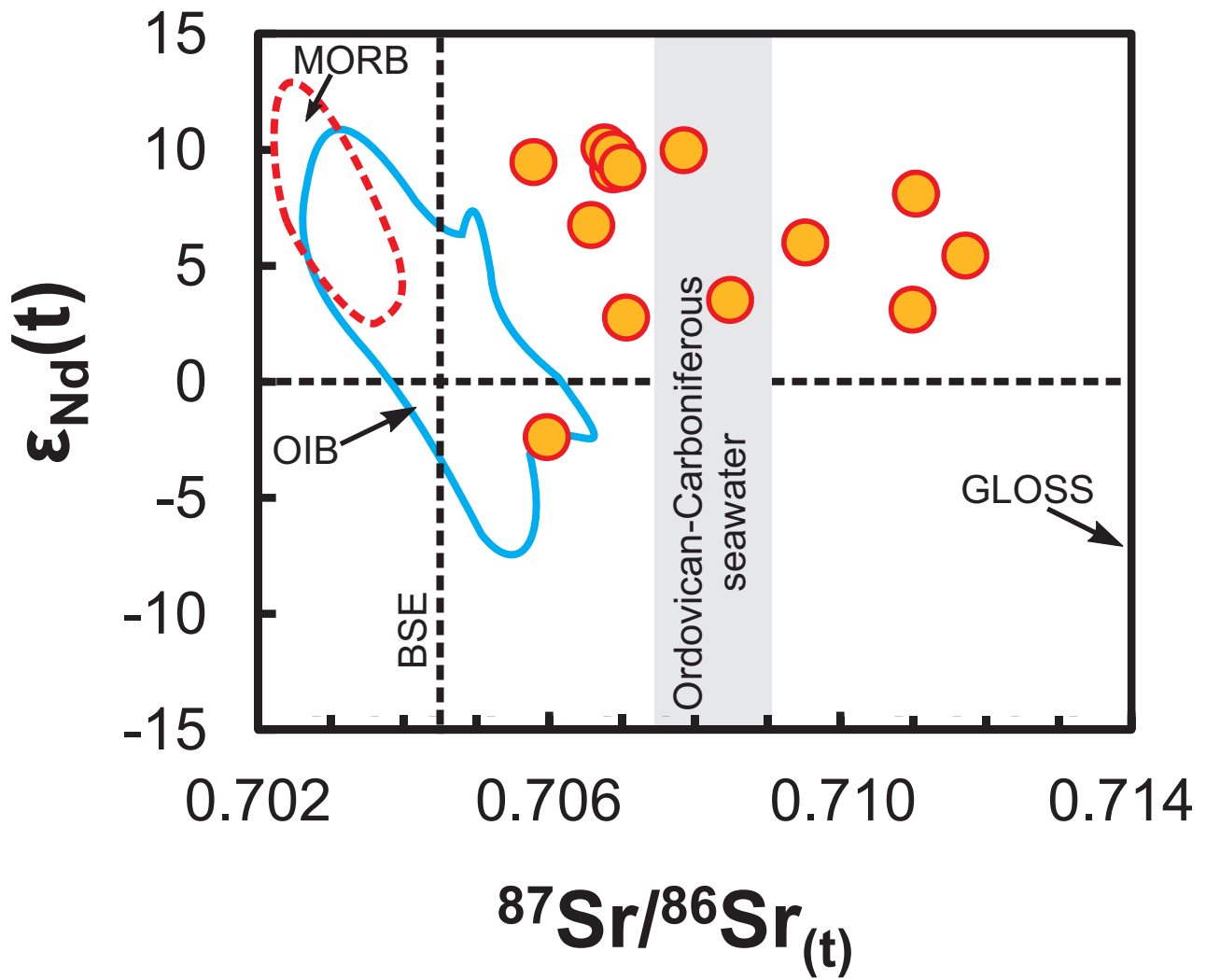
Figure. 1 Wang et al.

Figure. 2 Wang et al.

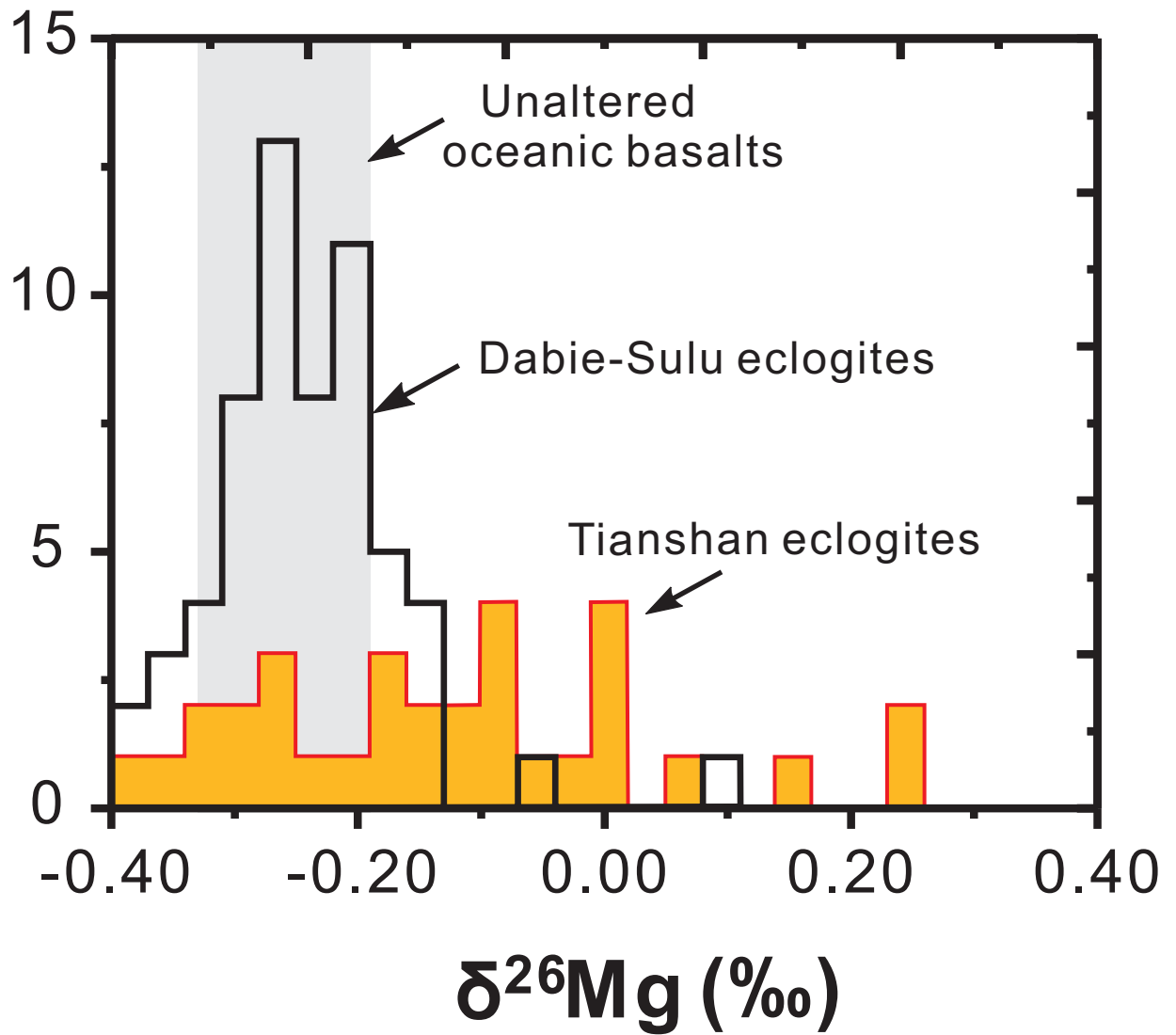


Figure. 3 Wang et al.

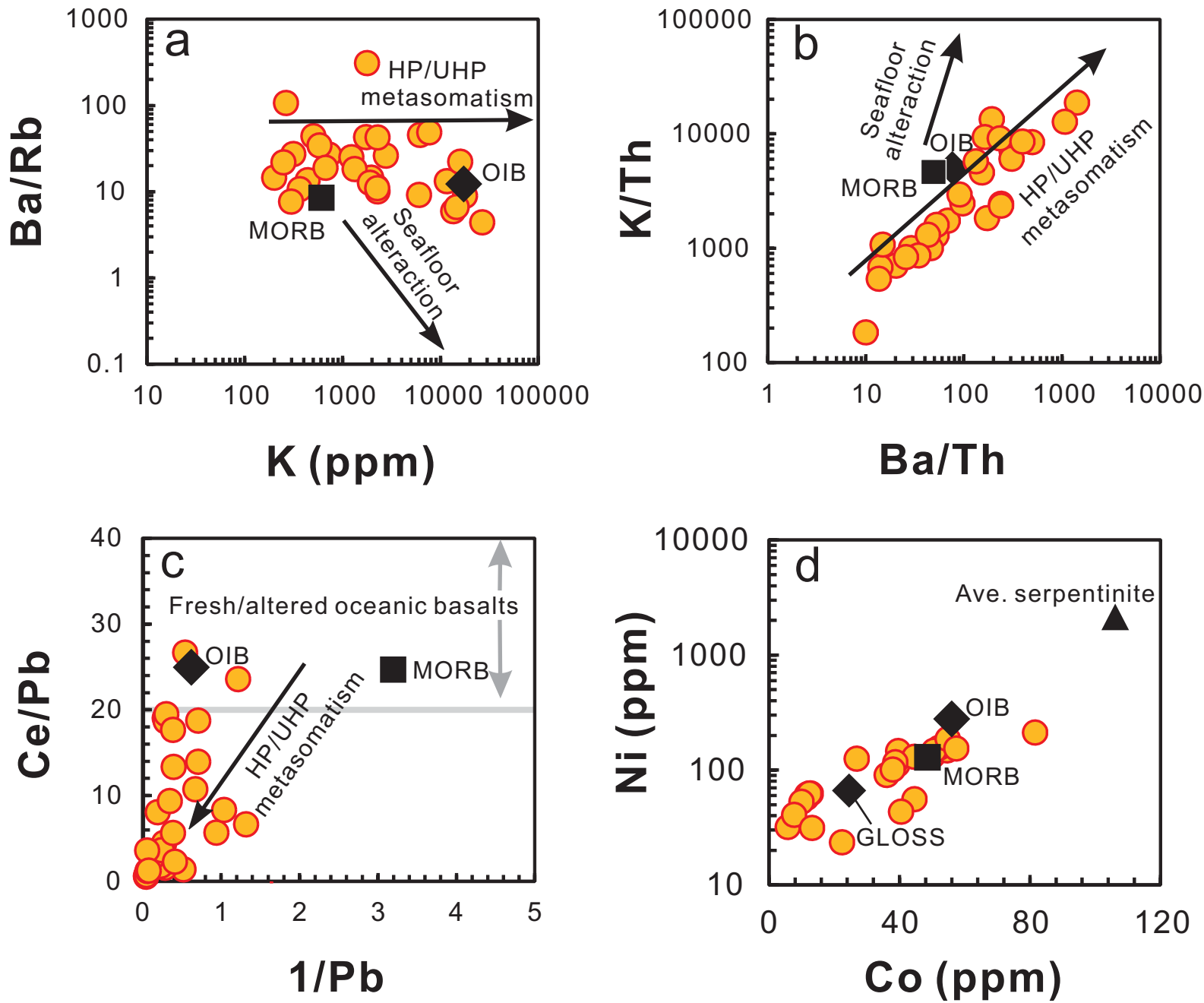


Figure. 4 Wang et al.

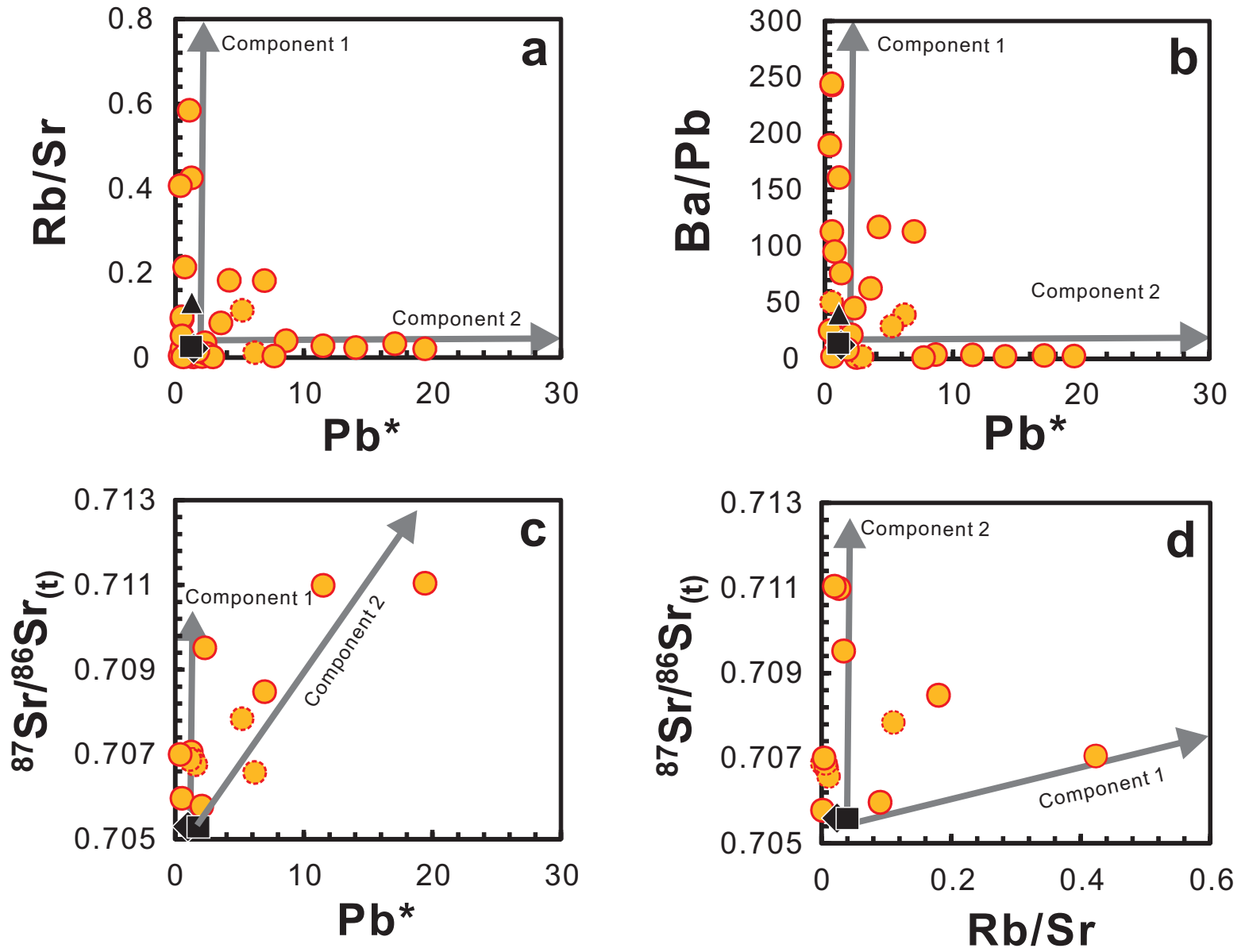


Figure. 5 Wang et al.

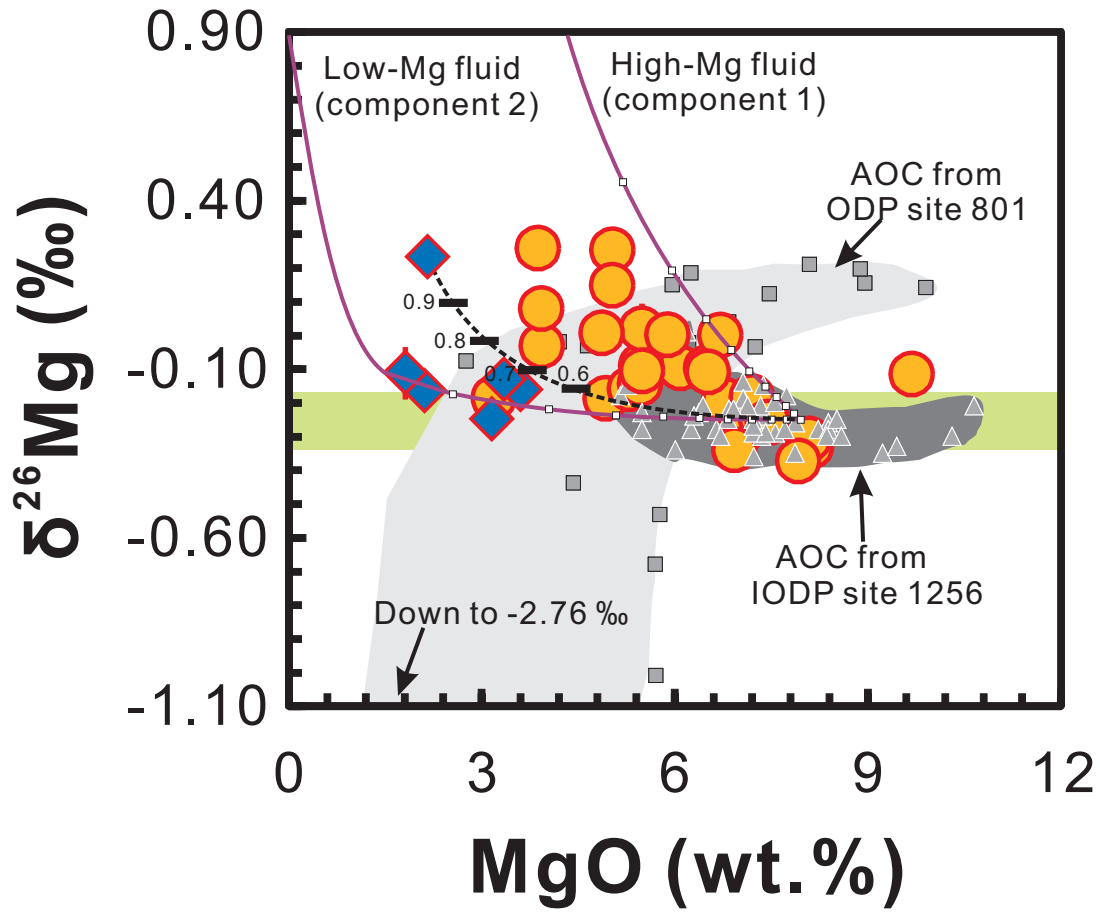
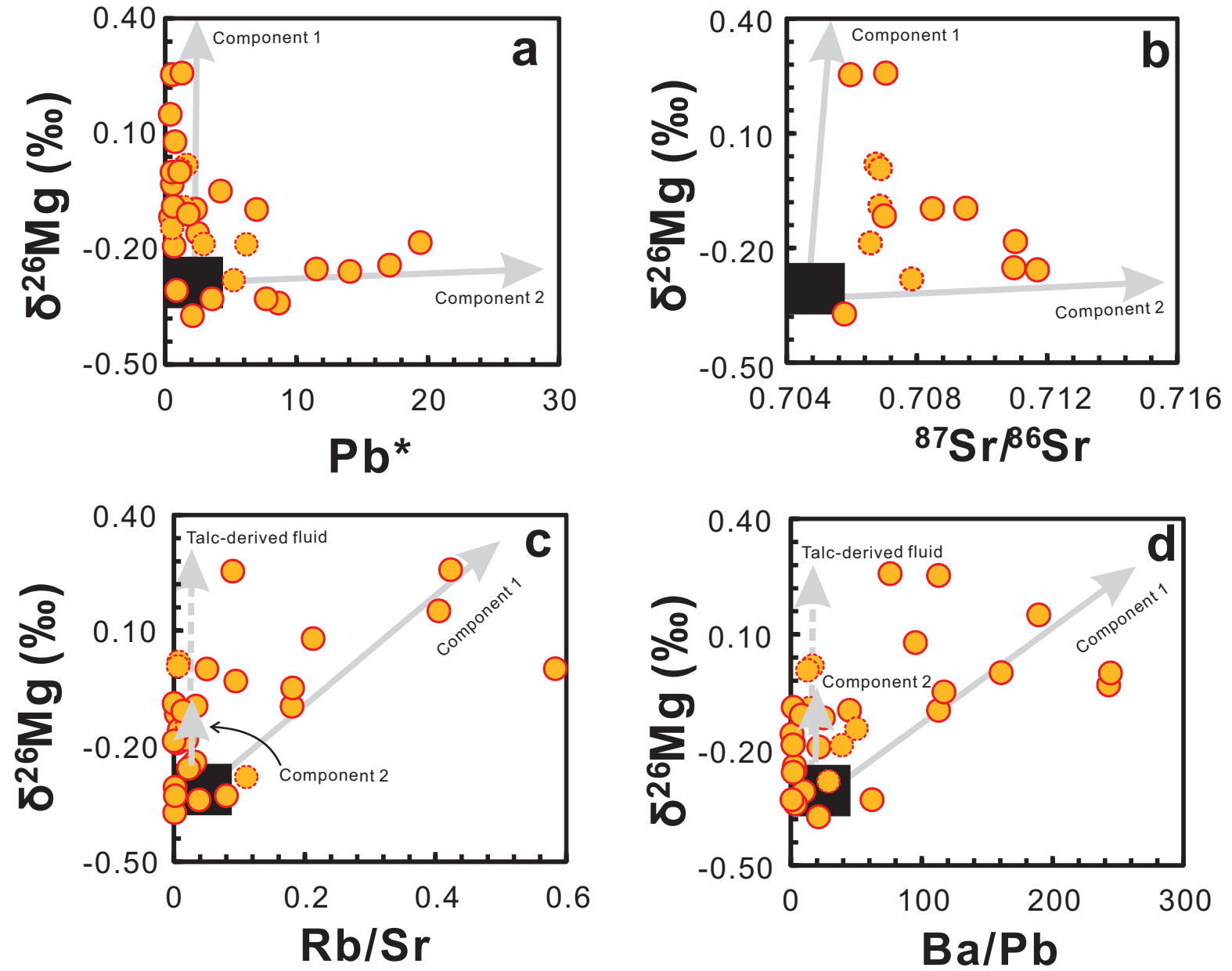


Figure. 6 Wang et al.



1 Table 1. Strontium and Nd isotopic compositions of the eclogites from southwestern Tianshan

2

Sample	Rb(ppm)	Sr(ppm)	⁸⁷ Rb/ ⁸⁶ Sr	⁸⁷ Sr/ ⁸⁶ Sr	2sigma	⁸⁷ Sr/ ⁸⁶ Sr _(320Ma)	Sm(ppm)	Nd(ppm)	¹⁴⁷ Sm/ ¹⁴⁴ Nd	¹⁴³ Nd/ ¹⁴⁴ Nd	2sigma	εNd _(320Ma)
H902-7	31.1	332	0.271	0.707198	0.000006	0.7060	9.35	37.6	0.150	0.512418	0.000007	-2.4
300-1	89.2	203	1.275	0.712858	0.000045	0.7071	5.74	23.1	0.150	0.512682	0.000011	2.8
H902-4	3.9	115	0.099	0.709964	0.000004	0.7095	3.35	11.5	0.176	0.512903	0.000016	6.0
H902-5	8.5	47.0	0.523	0.710863	0.000004	0.7085	0.67	1.94	0.207	0.512841	0.000026	3.5
305-1 ^a	0.8	92.3	0.024	0.706988	0.000006	0.7069	1.51	4.47	0.204	0.513122	0.000012	9.2
305-2 ^a	1.4	181	0.022	0.706855	0.000006	0.7068	2.01	5.46	0.222	0.513209	0.000016	10.1
305-3 ^a	9.1	273	0.097	0.707012	0.000007	0.7066	1.32	4.23	0.188	0.512966	0.000024	6.8
305-4 ^a	5.0	42.8	0.338	0.709384	0.000008	0.7078	2.4	6.56	0.221	0.513201	0.000016	10.0
X3-1 ^a	1.1	175	0.018	0.706961	0.000008	0.7069	2.43	6.92	0.212	0.513172	0.000007	9.8
8-12	4.0	297	0.039	0.711889	0.000008	0.7117	3.09	9.50	0.196	0.512917	0.000009	5.4
H608-6	5.4	149	0.105	0.711467	0.000003	0.7110	3.14	10.2	0.186	0.512775	0.000019	3.1
8-4	2.6	128	0.058	0.711301	0.000007	0.7110	2.34	7.37	0.191	0.513043	0.000034	8.1
8-9	0.4	112	0.011	0.707053	0.000004	0.7070	3.92	13.2	0.179	0.513076	0.000013	9.2
8-20	4.4	170	0.075	0.706122	0.000007	0.7058	5.11	16.3	0.189	0.513108	0.000017	9.5

3 Note: Samples marked with a superscript “a” are carbonated eclogites enclosed in marbles, and all the others are the eclogites enclosed in mica schists

4

5 Table 2. Magnesium isotopic compositions of the eclogites and mica schists and their mineral
 6 separates from southwestern Tianshan.

Sample	Rock/Mineral	$\delta^{26}\text{Mg}$	2SD	$\delta^{25}\text{Mg}$	2SD
<i>Eclogites/blueschists</i>					
H902-7	Bulk rock	0.27	0.08	0.16	0.05
	Replicate	0.24	0.06	0.14	0.08
	average	0.25	0.05	0.15	0.04
	Grt	-1.37	0.07	-0.69	0.06
	Cpx	0.46	0.07	0.27	0.06
300-1	Bulk rock	0.25	0.05	0.16	0.04
	Replicate	0.28	0.07	0.15	0.05
	average	0.26	0.04	0.16	0.04
H902-4	Bulk rock	-0.10	0.05	-0.03	0.04
	Grt	-1.61	0.07	-0.88	0.06
	Duplicate	-1.70	0.07	-0.87	0.05
	average	-1.66	0.05	-0.87	0.04
	Cpx	0.09	0.05	0.02	0.07
	Replicate	0.05	0.05	0.04	0.07
	average	0.07	0.04	0.03	0.05
H902-5	Bulk rock	-0.10	0.06	-0.04	0.05
	Grt	-1.58	0.07	-0.78	0.07
	Duplicate	-1.47	0.09	-0.77	0.06
	average	-1.54	0.06	-0.78	0.04
	Cpx	0.06	0.05	0.01	0.07
H907-21	Bulk rock	-0.19	0.06	-0.11	0.05
	Grt	-1.45	0.09	-0.76	0.06
	Cpx	-0.04	0.05	-0.05	0.07
305-1 ^a	Bulk rock	-0.09	0.05	-0.07	0.05
	Grt	-1.10	0.07	-0.58	0.05
	Cpx	0.14	0.07	0.09	0.05
305-2 ^a	Bulk rock	0.02	0.08	0.02	0.05
	Grt	-1.17	0.06	-0.60	0.05
	Duplicate	-1.16	0.06	-0.64	0.05
	Replicate	-1.16	0.09	-0.59	0.06
	average	-1.16	0.04	-0.62	0.03
	Cpx	0.11	0.07	0.04	0.05
305-3 ^a	Bulk rock	-0.19	0.06	-0.10	0.03
305-4 ^a	Bulk rock	-0.28	0.05	-0.16	0.04
X3-1 ^a	Bulk rock	0.01	0.06	-0.01	0.05
	Grt	-1.16	0.06	-0.63	0.04
	Duplicate	-1.15	0.09	-0.60	0.06
	average	-1.16	0.05	-0.62	0.03
8-12	Bulk rock	-0.26	0.05	-0.13	0.04

8-19	Bulk rock	-0.33	0.05	-0.19	0.05
	Grt	-1.54	0.07	-0.79	0.06
	Replicate	-1.52	0.06	-0.75	0.06
	Duplicate	-1.51	0.07	-0.80	0.06
	average	-1.52	0.04	-0.78	0.03
	Cpx	0.27	0.07	0.13	0.05
8-26	Bulk rock	-0.31	0.05	-0.16	0.05
H608-6	Bulk rock	-0.25	0.05	-0.11	0.04
	Grt	-1.56	0.07	-0.81	0.05
8-3	Bulk rock	-0.24	0.05	-0.13	0.04
	Grt	-1.51	0.09	-0.83	0.06
8-4	Bulk rock	-0.17	0.05	-0.10	0.05
	Replicate	-0.19	0.06	-0.09	0.05
	average	-0.18	0.04	-0.10	0.04
	Grt	-1.67	0.07	-0.87	0.07
	Duplicate	-1.65	0.09	-0.87	0.06
	average	-1.66	0.06	-0.87	0.04
8-5	Bulk rock	-0.26	0.05	-0.13	0.04
	Grt	-1.34	0.07	-0.70	0.06
8-7	Bulk rock	-0.34	0.06	-0.15	0.05
8-9	Bulk rock	-0.12	0.06	-0.05	0.05
8-20	Bulk rock	-0.37	0.05	-0.16	0.05
	Grt	-1.75	0.07	-0.89	0.05
	Cpx	-0.02	0.07	-0.03	0.05
H710-3	Bulk rock	-0.16	0.05	-0.03	0.05
A314-3 ^a	Bulk rock	-0.15	0.08	-0.08	0.05
	Grt	-1.53	0.07	-0.80	0.05
	Cpx	0.45	0.05	0.26	0.07
105-1	Bulk rock	-0.03	0.07	-0.03	0.06
105-12	Bulk rock	0.00	0.07	0.02	0.06
106-14 ^a	Bulk rock	-0.19	0.07	-0.12	0.06
110-3	Bulk rock	0.08	0.07	0.01	0.06
Q316-10	Bulk rock	-0.09	0.04	-0.04	0.02
A300-3	Bulk rock	0.00	0.03	0.00	0.03
a300-16	Bulk rock	-0.11	0.04	-0.05	0.02
H902-10	Bulk rock	-0.33	0.02	-0.16	0.02
k984 - 1	Bulk rock	-0.05	0.06	-0.02	0.03
H902-2 - 1	Bulk rock	0.15	0.01	0.07	0.01
<u>Mica schist</u>					
106-3B	Bulk rock	-0.18	0.07	-0.08	0.06
	Duplicate	-0.13	0.08	-0.05	0.05
	average	-0.16	0.05	-0.06	0.04
986-1	Bulk rock	-0.11	0.08	-0.02	0.05
305-5	Bulk rock	-0.16	0.05	-0.08	0.04

Q314-1	Bulk rock	0.23	0.02	0.13	0.03
Q316-4	Bulk rock	-0.25	0.02	-0.13	0.01
H865 - 1	Bulk rock	-0.13	0.03	-0.06	0.01

7 Note:

8 Samples marked with a superscript "a" are carbonated eclogites enclosed in marbles, and all the

9 others are the eclogites enclosed in mica schists; Grt = garnet; Cpx = clinopyroxene;

10 2SD = two times the standard deviation of the population of n (n>20) repeat measurements of the
11 standard during an analytical session;

12 Replicate: repeat sample dissolution, column chemistry and instrument analysis of Mg isotopic ratios;

13 Duplicate: repeat measurement of Mg isotopic ratios on the same solution.

LaTeX Source Files

[Click here to download LaTeX Source Files: 2017 June 20_Supplement.docx](#)